Progress In Electromagnetics Research B, Vol. 77, 117–136, 2017

Harmonically Time Varying, Traveling Electromagnetic Fields along a Plate and a Laminate with a Rectangular Cross Section, Isotropic Materials and Infinite Length

Birger Marcusson* **and Urban Lundin**

Abstract—This article contains derivation of propagation factors and Fourier series for harmonically time varying, traveling electromagnetic fields in a plate and a laminate with rectangular cross sections, isotropic materials and infinite length. Different and quite general fields are taken into account on all boundaries. Choices of boundary conditions and continuity conditions are discussed. Certain combinations of types of boundary conditions make the derivation possible for a laminate. Comparisons are made between results of Fourier series and finite element calculations.

1. INTRODUCTION

Results from measurements or calculations of magnetic or electric field on the boundary of a plate or laminate can be used for calculations of the electromagnetic fields within the plate or laminate. This is the main motive for the work presented in this article. Furthermore, analytical formulas can give information about how material properties and geometrical parameters affect the electromagnetic fields. An overview of analytical methods for calculation of magnetic fields are given by [1]. An integral equation method [2] and the stream function method [3] have been suggested for estimation of eddy currents in a plate where reaction fields have been neglected. Mukerji et al. have used Fourier's method, also called the method of separation of variables, in analyses of electromagnetic fields in a plate [4], and a laminate [5, 6]. In [4] and [5], the magnetic field is assumed to be alternating as in a transformer. In [6], traveling fields, simplified boundary conditions and no magnetic field in the stacking direction on the boundary are assumed. However, in the end regions of a plate package and the end regions of the stator core of an electric machine, the magnetic field in the stacking direction can be significant for the eddy current loss because of the large plate surfaces without interruptions of eddy currents.

The subject of this article is to use Fourier's method to derive analytical expressions for propagation factors, traveling magnetic and electric field components in a plate and a laminate. The boundary conditions are more general than in previous publications. The results are also approximately valid for hollow cylindrical laminates such that the fundamental wave length is much shorter than the circumference of the cylinder. Applications where linear or cylindrical laminates can be of interest are magnetic cores in electrical machines, magnetic shielding, rail guns and rails for magnetic levitation. In a synchronous generator, the field waves could be generated by the motion of magnetic poles of alternating polarities, and the laminate could be a simplified stator core.

Harmonically time varying electromagnetic fields are studied in this article. Therefore, the equations are written in complex form. This allows the time dependence to be removed from the equations. A real, time dependent field is the real or imaginary part of the product of the time

Received 19 June 2017, Accepted 18 July 2017, Scheduled 29 July 2017
* Corresponding author: Birger Marcusson (birger.marcusson@angstrom.uu.se).
The authors are with the Division for Electricity, Department of Engineering Sciences, Uppsala University, Box 534, SE-751 21 Uppsala, Sweden.

independent complex solution and $e^{j(\omega t+\Phi)}$ where $j=\sqrt{-1}$, t is the time, and Φ is a reference phase angle. All field components have Φ in common. It is chosen according to the initial conditions. Above a letter,$^{-}$ denotes a complex quantity,$^{\sim}$ denotes a Fourier coefficient, and $\hat{}$ denotes an amplitude. Vectors and matrices are denoted by bold letters.

Section 2 starts with fundamental equations and assumptions. In Section 2.1, Fourier series for components of magnetic field strength, $\bar{\mathbf{H}}$, and electric field strength, $\bar{\mathbf{E}}$, in one plate are derived. The choice of type of boundary conditions is discussed, and alternative expressions of eddy current loss density, p, and $\bar{\mathbf{E}}$ components are given. Section 2.1.1 contains derivation of the propagation factors. In Section 2.2, Fourier series for $\bar{\mathbf{H}}$ and $\bar{\mathbf{E}}$ components in a laminate of two plates are derived. After a discussion that leads to continuity conditions, Section 2.2 proceeds with a choice of boundary conditions for each plate. The Fourier series of $\bar{\mathbf{H}}$ and $\bar{\mathbf{E}}$ components containing both the known and the unknown Fourier coefficients are derived and used in continuity equations expressed per mode. Finally, these equations are solved with respect to the unknown Fourier coefficients. In Section 2.2.1, equations for Fourier coefficients of Neumann boundary functions are derived. In Section 2.3, equation systems for the Fourier coefficients of the internal boundary functions in the case of an arbitrary number of material layers are presented without solution. Section 3 describes comparisons between Fourier series and finite element analyses (FEA). First, the methods are described. Finally, results from Fourier series and FEA are shown in graphs. In Section 4, surface current density and the influence of lamination on the field components are discussed.

2. DERIVATION OF HARMONICALLY TIME VARYING ELECTROMAGNETIC FIELDS

In all studied cases, the z direction is the stacking direction, and the laminate has infinite extension in the x direction. Electromagnetic waves with only one angular frequency, ω, and wave length, λ, in the x direction are assumed to sweep along the laminate in the x direction. The wave propagation constant in the x direction is

$$k=\frac{2\pi}{\lambda} \tag{1}$$

Maxwell's equations in complex form are

$$\nabla\cdot\left(\varepsilon\bar{\mathbf{E}}\right) = \rho, \tag{2}$$

$$\nabla\cdot\bar{\mathbf{B}} = 0, \tag{3}$$

$$\nabla\times\bar{\mathbf{E}} = -j\omega\bar{\mathbf{B}}, \tag{4}$$

$$\nabla\times\bar{\mathbf{H}} = \bar{\mathbf{J}}+j\omega\varepsilon\bar{\mathbf{E}} \tag{5}$$

where ε is the permittivity, ρ the volume charge density, $\bar{\mathbf{B}}$ the magnetic flux density, and $\bar{\mathbf{J}}$ the current density. With permeability, μ, and conductivity, σ, the relationships assumed between $\bar{\mathbf{B}}$ and $\bar{\mathbf{H}}$, and between $\bar{\mathbf{J}}$ and $\bar{\mathbf{E}}$ are

$$\bar{\mathbf{B}} = \mu\bar{\mathbf{H}}, \tag{6}$$

$$\bar{\mathbf{J}} = \sigma\bar{\mathbf{E}}. \tag{7}$$

In general, ε, μ, and σ are tensors. For isotropic materials they are scalars.

2.1. One Rectangular, Infinitely Long, Isotropic Plate

Figure 1 shows the geometry and assumed coordinate system of a plate with width W and thickness T. The properties ε, μ, and σ are assumed to be constant. Equations (3) to (7) give that the i component of Eq. (4) multiplied by $\sigma+j\omega\varepsilon$ can be written as the wave equation

$$\frac{\partial^2\bar{H}_i}{\partial x^2}+\frac{\partial^2\bar{H}_i}{\partial y^2}+\frac{\partial^2\bar{H}_i}{\partial z^2}=\bar{\gamma}^2\bar{H}_i,\ i=x,y \text{ or } z \tag{8}$$

where $\bar{\gamma}^2$ is given by

$$\bar{\gamma}^2=-\omega^2\mu\varepsilon+j\omega\mu\sigma. \tag{9}$$

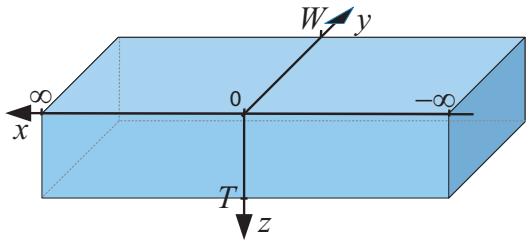

Figure 1. Plate with thickness T, width W and infinite extension in the x direction.

Wave equations for the components of $\bar{\mathbf{E}}$ have the same form as Eq. (8) and the same $\bar{\gamma}$. For derivation of wave equations for the components of $\bar{\mathbf{E}}$ in an uncharged medium, Eq. (2) with $\rho = 0$ would be used instead of Eq. (3). The periodic boundary conditions are

$$\bar{H}_i(x,y,z) = \bar{H}_i(x+\lambda,y,z) \quad \frac{\partial \bar{H}_i(x,y,z)}{\partial x} = \frac{\partial \bar{H}_i(x+\lambda,y,z)}{\partial x}, \quad i = x,y \text{ or } z. \tag{10}$$

Equation (8) with boundary conditions can be solved with Fourier's method if $\bar{H}_i$ is written as the sum of two contributions, $\bar{H}_{i1}$ and $\bar{H}_{i2}$. Here, $\bar{H}_{i1}$ has its inhomogeneous boundary conditions at $z = 0$ and $z = T$, and $\bar{H}_{i2}$ has its inhomogeneous boundary conditions at $y = 0$ and $y = W$. Each term in the Fourier series of $\bar{H}_{i1}$ is of the form $\bar{X}_m(x)Y_n(y)\bar{\bar{Z}}_{m,n}(z)$ where $\bar{\bar{Z}}_{m,n}(z)$ is a Fourier coefficient, and the other functions are eigenfunctions. As shown below, also $\bar{\bar{Z}}_{m,n}(z)$ could be regarded as some kind of eigenfunction considering the type of equation it satisfies. With use of the Fourier series of $\bar{H}_{i1}$, Eq. (8) can be written as a Fourier series that is zero everywhere. Because of the orthogonality of the eigenfunctions, each Fourier coefficient can be extracted, one by one, from the Fourier series. This is done by multiplication of the Fourier series by the eigenfunction that corresponds to the Fourier coefficient and then integration over the domain of the eigenfunction. Such extraction of the Fourier coefficients gives that all Fourier coefficients are zero in a Fourier series that is zero in every point. It implies that

$$\frac{\bar{X}_m''}{\bar{X}_m} + \frac{Y_n''}{Y_n} + \frac{\bar{\bar{Z}}_{m,n}''}{\bar{\bar{Z}}_{m,n}} = \bar{\gamma}^2, \tag{11}$$

and that every term in $\bar{H}_{i1}$ also satisfies Eq. (8). All terms on the left-hand side must be constants since they are independent and have a constant sum. Equation (11) can therefore be separated into the three equations

$$\bar{X}_m''(x) + \vartheta_m^2 \bar{X}_m(x) = 0, \qquad Y_n''(y) + K_n^2 Y_n(y) = 0, \qquad \bar{\bar{Z}}_{m,n}''(z) = \bar{\eta}_{m,n}^2 \bar{\bar{Z}}_{m,n}(z) \tag{12}$$

where ϑ_m, K_n and $\bar{\eta}_{m,n}$ are eigenvalues, but $\bar{\eta}_{m,n}$ is referred to as a propagation factor below. Insertion of Eq. (12) into Eq. (11) gives

$$\bar{\eta}_{m,n}^2 = \bar{\gamma}^2 + \vartheta_m^2 + K_n^2. \tag{13}$$

The general solution of the last equation (12) is

$$\bar{\bar{Z}}_{i,m,n}(z) = \bar{C}_{i,m,n} e^{\bar{\eta}_{m,n} z} + \bar{D}_{i,m,n} e^{-\bar{\eta}_{m,n} z}, \quad i = x,y \text{ or } z \tag{14}$$

where subscript i has been added to mark that the Fourier coefficients are different for different components of $\bar{\mathbf{H}}$. An arbitrary term in a Fourier series of $\bar{H}_{i2}$ can be written as $\bar{X}_m(x)\bar{\bar{Y}}_{l,m}(y)Z_l(z)$ where $\bar{\bar{Y}}_{l,m}(y)$ is a Fourier coefficient, and the other functions are eigenfunctions. As for $\bar{H}_{i1}$, to require $\bar{H}_{i2}$ to satisfy Eq. (8) implies that an arbitrary term in the Fourier series also satisfies Eq. (8). That gives

$$\frac{\bar{X}_m''}{\bar{X}_m} + \frac{\bar{\bar{Y}}_{l,m}''}{\bar{\bar{Y}}_{l,m}} + \frac{Z_l''}{Z_l} = \bar{\gamma}^2. \tag{15}$$

Equation (15) can be separated into

$$\bar{X}_m''(x) + \vartheta_m^2 \bar{X}_m(x) = 0, \qquad Z_l''(z) + \kappa_l^2 Z_l(z) = 0, \qquad \bar{\bar{Y}}_{l,m}''(y) = \bar{\nu}_{l,m}^2 \bar{\bar{Y}}_{l,m}(y) \tag{16}$$

where κ_l and $\bar{\nu}_{l,m}$ are eigenvalues, but $\bar{\nu}_{l,m}$ is referred to as a propagation factor. Insertion of Eq. (16) into Eq. (15) gives

$$\bar{\nu}_{l,m}^2 = \bar{\gamma}^2 + \vartheta_m^2 + \kappa_l^2. \tag{17}$$

The general solution of the last equation (16) is

$$\bar{\bar{Y}}_{i,l,m}(y) = \bar{C}_{i,l,m} e^{\bar{\nu}_{l,m} y} + \bar{D}_{i,l,m} e^{-\bar{\nu}_{l,m} y}, \quad i = x, y \text{ or } z. \tag{18}$$

For given harmonically time varying electromagnetic fields on a boundary, the type of boundary conditions can be chosen arbitrarily among Dirichlet, Neumann and Robin conditions. The choice affects the eigenfunctions and analytical expressions but not the numerical values of the sum of the Fourier series of $\bar{H}_{i1}$ and $\bar{H}_{i2}$ except, possibly, exactly on the edges. There, the Fourier sums may not converge to the field component. The Fourier sums converge slowly if the field component and eigenfunctions do not satisfy the same Dirichlet conditions. This gives rise to the Gibbs phenomenon at the edges [7]. For simplicity, in spite of slow convergence, Dirichlet conditions are here used on all surfaces where y or z is constant. The Dirichlet conditions for $\bar{H}_{i1}$ are

$$\bar{H}_{i1}(x,0,z) = 0, \qquad \bar{H}_{i1}(x,W,z) = 0, \ i = x, y \text{ or } z, \tag{19}$$

$$\bar{H}_{i1}(x,y,0) = \bar{H}_i(x,y,0) = \bar{f}_i^{z=0}(y) e^{-jkx}, \qquad \bar{H}_{i1}(x,y,T) = \bar{H}_i(x,y,T) = \bar{f}_i^{z=T}(y) e^{-jkx} \tag{20}$$

where $i = x$, y or z. The Dirichlet conditions for $\bar{H}_{i2}$ are

$$\bar{H}_{i2}(x,0,z) = \bar{H}_i(x,0,z) = \bar{f}_i^{y=0}(z) e^{-jkx}, \qquad \bar{H}_{i2}(x,W,z) = \bar{H}_i(x,W,z) = \bar{f}_i^{y=W}(z) e^{-jkx}, \tag{21}$$

$$\bar{H}_{i2}(x,y,0) = 0, \qquad \bar{H}_{i2}(x,y,T) = 0, \ i = x, y \text{ or } z \tag{22}$$

where $\bar{f}_i^{z=0}$, $\bar{f}_i^{z=T}$, $\bar{f}_i^{y=0}$ and $\bar{f}_i^{y=W}$ are boundary functions. The first equation (12) and the periodic conditions in Eq. (10) are satisfied by the eigenfunctions

$$\bar{X}_m(x) = e^{j\vartheta_m x}, \ \vartheta_m = mk, \ m = \ldots, -2, -1, 0, 1, 2, \ldots. \tag{23}$$

Equation (19) and the second equation in Eq. (12) are satisfied by the eigenfunctions

$$Y_n(y) = \sin K_n y, \ K_n = \frac{n\pi}{W}, \ n = 1, 2, 3, \ldots. \tag{24}$$

Equation (22) and the second equation in Eq. (16) are satisfied by the eigenfunctions

$$Z_l(z) = \sin \kappa_l z, \ \kappa_l = \frac{l\pi}{T}, \ l = 1, 2, 3, \ldots. \tag{25}$$

A Fourier series of $\bar{H}_{i1}$ with Fourier coefficients from Eq. (14) and eigenfunctions from Eqs. (23) and (24) is

$$\bar{H}_{i1}(x,y,z) = \sum_{n=1}^{\infty} \sum_{m=-\infty}^{\infty} \left(\bar{C}_{i,m,n} e^{\bar{\eta}_{m,n} z} + \bar{D}_{i,m,n} e^{-\bar{\eta}_{m,n} z} \right) e^{jmkx} \sin K_n y, \ i = x, y \text{ or } z. \tag{26}$$

Since the boundary conditions contain only one of the x dependent eigenfunctions, subscript m can be skipped, and Eq. (26) is reduced to

$$\bar{H}_{i1}(x,y,z) = e^{-jkx} \sum_{n=1}^{\infty} \left(\bar{C}_{i,n} e^{\bar{\eta}_n z} + \bar{D}_{i,n} e^{-\bar{\eta}_n z} \right) \sin K_n y, \ i = x, y \text{ or } z. \tag{27}$$

Similarly, a Fourier series of $\bar{H}_{i2}$ with Fourier coefficients from Eq. (18) and eigenfunctions from Eqs. (25) and (23) with $m = -1$ is

$$\bar{H}_{i2}(x,y,z) = e^{-jkx} \sum_{l=1}^{\infty} \left(\bar{C}_{i,l} e^{\bar{\nu}_l y} + \bar{D}_{i,l} e^{-\bar{\nu}_l y} \right) \sin \kappa_l z, \ i = x, y \text{ or } z. \tag{28}$$

Fourier series of the inhomogeneous Dirichlet boundary conditions in Eqs. (20) and (21) are

$$\bar{H}_{i1}(x,y,0)=e^{-jkx}\sum_{n=1}^{\infty}\bar{\bar{f}}_{i,n}^{z=0}\sin K_n y,\qquad \bar{H}_{i1}(x,y,T)=e^{-jkx}\sum_{n=1}^{\infty}\bar{\bar{f}}_{i,n}^{z=T}\sin K_n y,\ i=x,y \text{ or } z, \tag{29}$$

$$\bar{H}_{i2}(x,0,z)=e^{-jkx}\sum_{l=1}^{\infty}\bar{\bar{f}}_{i,l}^{y=0}\sin \kappa_l z,\qquad \bar{H}_{i2}(x,W,z)=e^{-jkx}\sum_{l=1}^{\infty}\bar{\bar{f}}_{i,l}^{y=W}\sin \kappa_l z,\ i=x,y \text{ or } z. \tag{30}$$

Term-by-term identification of Eq. (23) with Eq. (29) at $z=0$ and $z=T$ gives

$$\bar{C}_{i,n}+\bar{D}_{i,n}=\bar{\bar{f}}_{i,n}^{z=0},\qquad \bar{C}_{i,n}e^{\bar{\eta}_n T}+\bar{D}_{i,n}e^{-\bar{\eta}_n T}=\bar{\bar{f}}_{i,n}^{z=T}. \tag{31}$$

Equation (31) gives

$$\bar{C}_{i,n}=\frac{\bar{\bar{f}}_{i,n}^{z=T}-\bar{\bar{f}}_{i,n}^{z=0}e^{-\bar{\eta}_n T}}{e^{\bar{\eta}_n T}-e^{-\bar{\eta}_n T}},\qquad \bar{D}_{i,n}=\frac{\bar{\bar{f}}_{i,n}^{z=0}e^{\bar{\eta}_n T}-\bar{\bar{f}}_{i,n}^{z=T}}{e^{\bar{\eta}_n T}-e^{-\bar{\eta}_n T}}. \tag{32}$$

Insertion of Eq. (32) into Eq. (27) gives

$$\bar{H}_{i1}(x,y,z)=e^{-jkx}\sum_{n=1}^{\infty}\left(\bar{\bar{f}}_{i,n}^{z=0}\sinh\bar{\eta}_n(T-z)+\bar{\bar{f}}_{i,n}^{z=T}\sinh\bar{\eta}_n z\right)\frac{\sin K_n y}{\sinh\bar{\eta}_n T},\ i=x,y \text{ or } z. \tag{33}$$

In the same way, Eqs. (28) and (30) give

$$\bar{H}_{i2}(x,y,z)=e^{-jkx}\sum_{l=1}^{\infty}\left(\bar{\bar{f}}_{i,l}^{y=0}\sinh\bar{\nu}_l(W-y)+\bar{\bar{f}}_{i,l}^{y=W}\sinh\bar{\nu}_l y\right)\frac{\sin \kappa_l z}{\sinh\bar{\nu}_l W},\ i=x,y \text{ or } z. \tag{34}$$

Equations (5), (33) and (34) give each $\bar{\mathbf{E}}$ component as a sum of two contributions, $\bar{E}_{i\eta}$ depending on η and $\bar{E}_{i\nu}$ depending on ν. These field components are

$$\begin{aligned}
\bar{E}_{x\eta}(x,y,z) &= \frac{e^{-jkx}}{\sigma+j\omega\varepsilon}\sum_{n=1}^{\infty}\frac{1}{\sinh\bar{\eta}_n T}\cdot\Big[\left(\bar{\bar{f}}_{z,n}^{z=0}\sinh\bar{\eta}_n(T-z)+\bar{\bar{f}}_{z,n}^{z=T}\sinh\bar{\eta}_n z\right)K_n\cos K_n y\\
&\quad+\bar{\eta}_n\left(\bar{\bar{f}}_{y,n}^{z=0}\cosh\bar{\eta}_n(T-z)-\bar{\bar{f}}_{y,n}^{z=T}\cosh\bar{\eta}_n z\right)\sin K_n y\Big], \qquad (35)\\
\bar{E}_{x\nu}(x,y,z) &= \frac{e^{-jkx}}{\sigma+j\omega\varepsilon}\sum_{l=1}^{\infty}\frac{1}{\sinh\bar{\nu}_l W}\cdot\Big[\bar{\nu}_l\left(\bar{\bar{f}}_{z,l}^{y=W}\cosh\bar{\nu}_l y-\bar{\bar{f}}_{z,l}^{y=0}\cosh\bar{\nu}_l(W-y)\right)\sin\kappa_l z\\
&\quad-\left(\bar{\bar{f}}_{y,l}^{y=0}\sinh\bar{\nu}_l(W-y)+\bar{\bar{f}}_{y,l}^{y=W}\sinh\bar{\nu}_l y\right)\kappa_l\cos\kappa_l z\Big], \qquad (36)\\
\bar{E}_{y\eta}(x,y,z) &= \frac{e^{-jkx}}{\sigma+j\omega\varepsilon}\sum_{n=1}^{\infty}\frac{\sin K_n y}{\sinh\bar{\eta}_n T}\cdot\Big[\bar{\eta}_n\left(\bar{\bar{f}}_{x,n}^{z=T}\cosh\bar{\eta}_n z-\bar{\bar{f}}_{x,n}^{z=0}\cosh\bar{\eta}_n(T-z)\right)\\
&\quad+jk\left(\bar{\bar{f}}_{z,n}^{z=0}\sinh\bar{\eta}_n(T-z)+\bar{\bar{f}}_{z,n}^{z=T}\sinh\bar{\eta}_n z\right)\Big], \qquad (37)\\
\bar{E}_{y\nu}(x,y,z) &= \frac{e^{-jkx}}{\sigma+j\omega\varepsilon}\sum_{l=1}^{\infty}\frac{1}{\sinh\bar{\nu}_l W}\cdot\Big[\left(\bar{\bar{f}}_{x,l}^{y=0}\sinh\bar{\nu}_l(W-y)+\bar{\bar{f}}_{x,l}^{y=W}\sinh\bar{\nu}_l y\right)\kappa_l\cos\kappa_l z\\
&\quad+jk\left(\bar{\bar{f}}_{z,l}^{y=0}\sinh\bar{\nu}_l(W-y)+\bar{\bar{f}}_{z,l}^{y=W}\sinh\bar{\nu}_l y\right)\sin\kappa_l z\Big], \qquad (38)\\
\bar{E}_{z\eta}(x,y,z) &= -\frac{e^{-jkx}}{\sigma+j\omega\varepsilon}\sum_{n=1}^{\infty}\frac{1}{\sinh\bar{\eta}_n T}\cdot\Big[jk\left(\bar{\bar{f}}_{y,n}^{z=0}\sinh\bar{\eta}_n(T-z)+\bar{\bar{f}}_{y,n}^{z=T}\sinh\bar{\eta}_n z\right)\sin K_n y\\
&\quad+\left(\bar{\bar{f}}_{x,n}^{z=0}\sinh\bar{\eta}_n(T-z)+\bar{\bar{f}}_{x,n}^{z=T}\sinh\bar{\eta}_n z\right)K_n\cos K_n y\Big], \qquad (39)\\
\bar{E}_{z\nu}(x,y,z) &= \frac{e^{-jkx}}{\sigma+j\omega\varepsilon}\sum_{l=1}^{\infty}\frac{\sin\kappa_l z}{\sinh\bar{\nu}_l W}\cdot\Big[-jk\left(\bar{\bar{f}}_{y,l}^{y=0}\sinh\bar{\nu}_l(W-y)+\bar{\bar{f}}_{y,l}^{y=W}\sinh\bar{\nu}_l y\right)\\
&\quad+\bar{\nu}_l\left(\bar{\bar{f}}_{x,l}^{y=0}\cosh\bar{\nu}_l(W-y)-\bar{\bar{f}}_{x,l}^{y=W}\cosh\bar{\nu}_l y\right)\Big]. \qquad (40)
\end{aligned}$$

The time average of the eddy current loss density is

$$p = \frac{1}{2}\bar{\mathbf{J}} \cdot \bar{\mathbf{E}}^* = \frac{\sigma}{2}\bar{\mathbf{E}} \cdot \bar{\mathbf{E}}^* = \frac{\sigma}{2}\left(\widehat{E}_x^2 + \widehat{E}_y^2 + \widehat{E}_z^2\right). \tag{41}$$

With Ampère's law, Eq. (5), the loss density can also be expressed as

$$\begin{aligned} p \;=\; & \frac{\sigma/2}{\sigma^2+\omega^2\varepsilon^2} \cdot \left(\frac{\partial \bar{H}_z}{\partial y}\frac{\partial \bar{H}_z^*}{\partial y} - 2\mathrm{Re}\left\{\frac{\partial \bar{H}_z}{\partial y}\frac{\partial \bar{H}_y^*}{\partial z}\right\} + \frac{\partial \bar{H}_y}{\partial z}\frac{\partial \bar{H}_y^*}{\partial z} + \frac{\partial \bar{H}_x}{\partial z}\frac{\partial \bar{H}_x^*}{\partial z} \right. \\ & \left. -2\mathrm{Re}\left\{\frac{\partial \bar{H}_x}{\partial z}\frac{\partial \bar{H}_z^*}{\partial x}\right\} + \frac{\partial \bar{H}_z}{\partial x}\frac{\partial \bar{H}_z^*}{\partial x} + \frac{\partial \bar{H}_y}{\partial x}\frac{\partial \bar{H}_y^*}{\partial x} - 2\mathrm{Re}\left\{\frac{\partial \bar{H}_y}{\partial x}\frac{\partial \bar{H}_x^*}{\partial y}\right\} + \frac{\partial \bar{H}_x}{\partial y}\frac{\partial \bar{H}_x^*}{\partial y}\right). \end{aligned} \tag{42}$$

According to Eq. (42), the loss density contributions from the $\bar{\mathbf{H}}$ components are coupled to each other unless the coupling terms are zero. Considering that the loss density can be expressed directly into the $\bar{\mathbf{E}}$ components, measuring $\bar{\mathbf{H}}$ to get the loss density in a single plate is a detour if $\bar{\mathbf{E}}$ can be measured. With boundary conditions specified for $\bar{\mathbf{E}}$ components, relatively simple Fourier series of the $\bar{\mathbf{E}}$ components can be derived in the same way as Eqs. (33) and (34). Only the boundary functions are different, g instead of f. Hence,

$$\bar{E}_{i1}(x,y,z) \;=\; e^{-jkx}\sum_{n=1}^{\infty}\left(\bar{\tilde{g}}_{i,n}^{z=0}\sinh\bar{\eta}_n(T-z) + \bar{\tilde{g}}_{i,n}^{z=T}\sinh\bar{\eta}_n z\right)\frac{\sin K_n y}{\sinh\bar{\eta}_n T},\;\; i=x,y \text{ or } z, \tag{43}$$

$$\bar{E}_{i2}(x,y,z) \;=\; e^{-jkx}\sum_{l=1}^{\infty}\left(\bar{\tilde{g}}_{i,l}^{y=0}\sinh\bar{\nu}_l(W-y) + \bar{\tilde{g}}_{i,l}^{y=W}\sinh\bar{\nu}_l y\right)\frac{\sin\kappa_l z}{\sinh\bar{\nu}_l W},\;\; i=x,y \text{ or } z. \tag{44}$$

2.1.1. Wave Propagation Factors $\bar{\eta}_n$ and $\bar{\nu}_l$

According to Eqs. (13) and (23) with $m=-1$, the real part, a_n, and imaginary part, b, of $\bar{\eta}_n^2$ are

$$a_n = k^2 + K_n^2 - \omega^2\mu\varepsilon, \qquad\qquad b = \omega\mu\sigma. \tag{45}$$

According to Eqs. (17) and (23) with $m=-1$, the real part, c_l, and imaginary part, d, of $\bar{\nu}_l^2$ are

$$c_l = k^2 + \kappa_l^2 - \omega^2\mu\varepsilon, \qquad\qquad d = \omega\mu\sigma. \tag{46}$$

Since the material is isotropic, $d=b$. The propagation factors can be expressed as

$$\bar{\eta}_n = \alpha_n + j\beta_n = \eta_n e^{j\theta_n}, \qquad\qquad \bar{\nu}_l = \xi_l + j\upsilon_l = \nu_l e^{j\Theta_l} \tag{47}$$

where α_n, β_n, θ_n, ξ_l, υ_l and Θ_l are real numbers. With Eq. (47), $\bar{\eta}_n^2$ can be expressed as

$$\bar{\eta}_n^2 = a_n + jb = \eta_n^2 e^{j2\theta_n} \tag{48}$$

where the angle $2\theta_n$ can be restricted to be between 0 and π since b is positive according to Eq. (45). There is no point in adding a multiple of 2π to $2\theta_n$. Consequently, $0 < \theta_n < \pi/2$. The real part of Eq. (48) is

$$\eta_n^2\cos 2\theta_n = a_n = \sqrt{a_n^2+b^2}\left(2\cos^2\theta_n - 1\right) \tag{49}$$

which with $0 < \theta_n < \pi/2$ gives

$$\cos\theta_n = \frac{1}{\sqrt{2}}\sqrt{1+\frac{a_n}{\sqrt{a_n^2+b^2}}}, \qquad\qquad \sin\theta_n = \frac{1}{\sqrt{2}}\sqrt{1-\frac{a_n}{\sqrt{a_n^2+b^2}}}. \tag{50}$$

With use of Eqs. (47) and (50), α_n and β_n can be written as

$$\alpha_n = \eta_n\cos\theta_n = \frac{1}{\sqrt{2}}\sqrt{\sqrt{a_n^2+b^2}+a_n}, \qquad \beta_n = \eta_n\sin\theta_n = \frac{1}{\sqrt{2}}\sqrt{\sqrt{a_n^2+b^2}-a_n}. \tag{51}$$

The real part ξ_l and imaginary part υ_l of $\bar{\nu}_l$ can be derived and written in the same way as α_n and β_n, i.e.

$$\xi_l = \nu_l\cos\Theta_l = \frac{1}{\sqrt{2}}\sqrt{\sqrt{c_l^2+d^2}+c_l}, \qquad \upsilon_l = \nu_l\sin\Theta_l = \frac{1}{\sqrt{2}}\sqrt{\sqrt{c_l^2+d^2}-c_l}. \tag{52}$$

2.2. A Laminate of Two Rectangular, Infinitely Long, Isotropic Material Layers

Figure 2 shows a cross section of a laminate with two material layers.

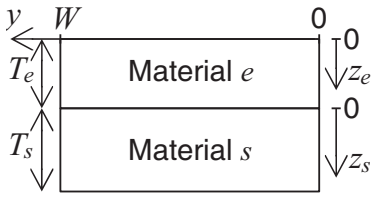

Figure 2. Cross section of a laminate with two material layers.

For a laminate, a distinction in this article is made between external and internal boundary functions. The domains of the external and internal boundary functions are within short distances from external and internal material interfaces, respectively. The $\bar{\mathbf{H}}$ and $\bar{\mathbf{E}}$ fields in a laminate on which only the field values on the outer laminate surfaces are known can be determined if the internal boundary functions can be determined. For comparisons with FEA, it is convenient to solve for $\bar{\mathbf{H}}$ first since $\bar{\mathbf{H}}$ is the primary unknown in the eddy current solver in ANSYS Maxwell. For $\bar{\mathbf{H}}$, there are six unknown boundary functions per material interface, one boundary function per $\bar{\mathbf{H}}$ component and side of the interface. The surface current density on material interfaces is assumed to be negligible for reasons given in Section 4. That combined with Ampère's law implies continuous tangential components of $\bar{\mathbf{H}}$ [8]. Furthermore, Faraday's law implies continuous tangential $\bar{\mathbf{E}}$ components. The continuity of tangential $\bar{\mathbf{E}}$ and $\bar{\mathbf{H}}$ components, in turn, implies continuity of the partial derivatives of the tangential $\bar{\mathbf{E}}$ and $\bar{\mathbf{H}}$ components with respect to any tangential coordinate. Six continuity conditions per material interface can be used for determination of the internal boundary functions. Together, one continuity condition per $\bar{\mathbf{H}}$ component and one per $\bar{\mathbf{E}}$ component are six conditions. However, these continuity conditions are not independent [9]. Faraday's law with the continuity of the tangential partial derivatives of the tangential $\bar{\mathbf{E}}$ components gives directly that the normal component of $\bar{\mathbf{B}}$ is continuous. Similarly, Ampère's law with the continuity of the tangential partial derivatives of the tangential $\bar{\mathbf{H}}$ components directly implies continuity of the normal component of the total current density, $\bar{\mathbf{J}}_{tot} = (\sigma + j\varepsilon)\bar{\mathbf{E}}$. Alternatively, the divergence of Ampère's law can be expressed as $\nabla \cdot \bar{\mathbf{J}}_{tot} = 0$, which together with the Divergence theorem can be used to show that the normal component of $\bar{\mathbf{J}}_{tot}$ is continuous. Simultaneous use of continuity conditions on $\bar{B}_z$, $\bar{E}_x$ and $\bar{E}_y$ can be meaningful when $\bar{\mathbf{E}}$ is not used in the continuity expression of $\bar{B}_z$. If, on the other hand, $\bar{E}_z$ is expressed in terms of $\bar{\mathbf{H}}$, as in Eqs. (39) and (40), a continuity condition on $\bar{J}_{tot,z}$ does not give anything useful not already given by continuity conditions on $\bar{H}_x$ and $\bar{H}_y$. Therefore, one more continuity condition is needed. Continuity conditions on $\bar{\mathbf{E}}$ components are ways to express continuity conditions on combinations of the partial derivatives of $\bar{\mathbf{H}}$ components. The only partial derivative of a $\bar{\mathbf{H}}$ component whose continuity at constant z is not implied by the other continuity conditions mentioned so far is $\frac{\partial \bar{H}_z}{\partial z}$. Continuity of $\frac{\partial \bar{H}_z}{\partial z}$ is implied by the combination of Eq. (3) and the continuity of $\frac{\partial \bar{H}_x}{\partial x}$ and $\frac{\partial \bar{H}_y}{\partial y}$ on an interface at constant z. With local z coordinates according to Fig. 2, the continuity conditions are

$$\bar{H}_{ei}(x, y, z_e = T_e) = \bar{H}_{si}(x, y, z_s = 0),\ i = x \text{ or } y, \tag{53}$$

$$\mu_e \bar{H}_{ez}(x, y, z_e = T_e) = \mu_s \bar{H}_{sz}(x, y, z_s = 0), \tag{54}$$

$$\frac{\partial \bar{H}_z}{\partial z}(x, y, z_e = T_e) = \frac{\partial \bar{H}_z}{\partial z}(x, y, z_s = 0), \tag{55}$$

$$\bar{E}_{ei}(x, y, z_e = T_e) = \bar{E}_{si}(x, y, z_s = 0),\ i = x \text{ or } y, \tag{56}$$

$$\bar{E}_{ez}(x, y, z_e = T_e) = \bar{q}\bar{E}_{sz}(x, y, z_s = 0) \tag{57}$$

where

$$\bar{q} \equiv \frac{\bar{\sigma}_s}{\bar{\sigma}_e}, \qquad \bar{\sigma}_i \equiv \sigma_i + j\omega\varepsilon_i, i = e \text{ or } s. \tag{58}$$

The valid but redundant continuity condition in Eq. (57) will not be used in this article. There is no need to solve for the Fourier coefficients appearing in Eqs. (43) and (44) if $\bar{\mathbf{E}}$ is expressed in terms of $\bar{\mathbf{H}}$. However, the orthogonality of the eigenfunctions cannot be used for obtaining the unknown Fourier coefficients in Eqs. (35) and (39) since these expressions contain eigenfunctions from different eigenfunction systems. Perhaps the simplest way to get rid of that obstacle is to use Neumann conditions instead of Dirichlet conditions for $\bar{H}_y$ at $y = 0$ and $y = W$. However, in this article the choice is to use Neumann conditions for $\bar{H}_x$ and $\bar{H}_z$ at $y = 0$ and $y = W$, and Neumann conditions for $\bar{H}_y$ on all boundaries that have a constant z. Thereby the sum of the Fourier series for each $\bar{\mathbf{H}}$ component does not have to be forced to zero on the edges by the sine eigenfunctions. For $i = x$ and z, and for an arbitrary plate in the laminate, the non-periodic boundary conditions, with valid Dirichlet conditions repeated for convenience, are

$$\frac{\partial \bar{H}_{i1}(x,0,z)}{\partial y} = 0, \qquad \frac{\partial \bar{H}_{i1}(x,W,z)}{\partial y} = 0, \tag{59}$$

$$\bar{H}_{i1}(x,y,0) = \bar{H}_i(x,y,0) = \bar{f}_i^{z=0}(y)e^{-jkx}, \qquad \bar{H}_{i1}(x,y,T) = \bar{H}_i(x,y,T) = \bar{f}_i^{z=T}(y)e^{-jkx}, \tag{20}$$

$$\frac{\partial \bar{H}_{i2}(x,0,z)}{\partial y} = \frac{\partial \bar{H}_i(x,0,z)}{\partial y} = \bar{F}_i^{y=0}(z)e^{-jkx}, \quad \frac{\partial \bar{H}_{i2}(x,W,z)}{\partial y} = \frac{\partial \bar{H}_i(x,W,z)}{\partial y} = \bar{F}_i^{y=W}(z)e^{-jkx}, \tag{60}$$

$$\bar{H}_{i2}(x,y,0) = 0, \qquad \bar{H}_{i2}(x,y,T) = 0. \tag{22}$$

The non-periodic boundary conditions for $\bar{H}_y$ are

$$\bar{H}_{y1}(x,0,z) = 0, \qquad \bar{H}_{y1}(x,W,z) = 0, \tag{19}$$

$$\frac{\partial \bar{H}_{y1}(x,y,0)}{\partial z} = \frac{\partial \bar{H}_y(x,y,0)}{\partial z} = \bar{F}_y^{z=0}(z)e^{-jkx}, \quad \frac{\partial \bar{H}_{y1}(x,y,T)}{\partial z} = \frac{\partial \bar{H}_y(x,y,T)}{\partial z} = \bar{F}_y^{z=T}(z)e^{-jkx}, \tag{61}$$

$$\bar{H}_{y2}(x,0,z) = \bar{H}_y(x,0,z) = \bar{f}_y^{y=0}(z)e^{-jkx}, \qquad \bar{H}_{y2}(x,W,z) = \bar{H}_y(x,W,z) = \bar{f}_y^{y=W}(z)e^{-jkx}, \tag{21}$$

$$\frac{\partial \bar{H}_{y2}(x,y,0)}{\partial z} = 0, \qquad \frac{\partial \bar{H}_{y2}(x,y,T)}{\partial z} = 0. \tag{62}$$

Eigenfunctions corresponding to Eq. (59) combined with Eq. (8) are

$$Y_n(y) = \cos K_n y, \ K_n = \frac{n\pi}{W}, \ n = 0,1,2,\ldots. \tag{63}$$

Eigenfunctions corresponding to Eq. (62) combined with Eq. (8) are

$$Z_l(z) = \cos \kappa_l z, \ \kappa_l = \frac{l\pi}{T}, \ l = 0,1,2,\ldots. \tag{64}$$

For $\bar{H}_{x1}$ and $\bar{H}_{z1}$, Eq. (32) is still valid since the boundary conditions at $z = 0$ and T are still Dirichlet conditions. The Fourier series of $\bar{H}_{i1}$ based on Eq. (59) and the Dirichlet conditions in Eq. (20) is

$$\bar{H}_{i1}(x,y,z) = e^{-jkx}\sum_{n=0}^{\infty}\left(\bar{\bar{f}}_{i,\mathrm{c},n}^{z=0}\sinh\bar{\eta}_n(T-z) + \bar{\bar{f}}_{i,\mathrm{c},n}^{z=T}\sinh\bar{\eta}_n z\right)\frac{\cos K_n y}{\sinh\bar{\eta}_n T}, \ i = x \text{ or } z. \tag{65}$$

where subscript c marks Fourier coefficients corresponding to cosine eigenfunctions. Fourier coefficients without subscript c correspond to sine eigenfunctions. The subscript is useful in equations that contain Fourier coefficients but no eigenfunctions. Sine Fourier series of the inhomogeneous Neumann boundary conditions in Eq. (60) are

$$\frac{\partial \bar{H}_{i2}(x,0,z)}{\partial y} = e^{-jkx}\sum_{l=1}^{\infty}\bar{\bar{F}}_{i,l}^{y=0}\sin\kappa_l z, \qquad \frac{\partial \bar{H}_{i2}(x,W,z)}{\partial y} = e^{-jkx}\sum_{l=1}^{\infty}\bar{\bar{F}}_{i,l}^{y=W}\sin\kappa_l z, \ i = x \text{ or } z. \tag{66}$$

The boundary condition in Eq. (60) combined with the Fourier series Eq. (28) gives a Fourier series that, because of the orthogonality, should be identical, term by term, to the Fourier series in Eq. (66). That gives

$$\bar{\nu}_l\left(\bar{C}_{i,l} - \bar{D}_{i,l}\right) = \bar{\bar{F}}_{i,l}^{y=0}, \qquad \bar{\nu}_l\left(\bar{C}_{i,l}e^{\bar{\nu}_l W} - \bar{D}_{i,l}e^{-\bar{\nu}_l W}\right) = \bar{\bar{F}}_{i,l}^{y=W}, \ i = x \text{ or } z. \tag{67}$$

Equation (67) gives

$$\bar{C}_{i,l} = \frac{\bar{\tilde{F}}_{i,l}^{y=W} - \bar{\tilde{F}}_{i,l}^{y=0} e^{-\bar{\nu}_l W}}{\bar{\nu}_l (e^{\bar{\nu}_l W} - e^{-\bar{\nu}_l W})}, \qquad \bar{D}_{i,l} = \frac{\bar{\tilde{F}}_{i,l}^{y=W} - \bar{\tilde{F}}_{i,l}^{y=0} e^{\bar{\nu}_l W}}{\bar{\nu}_l (e^{\bar{\nu}_l W} - e^{-\bar{\nu}_l W})}, \ i = x \text{ or } z. \tag{68}$$

Insertion of Eq. (68) into Eq. (28) gives

$$\bar{H}_{i2}(x,y,z) = e^{-jkx} \sum_{l=1}^{\infty} \left(\bar{\tilde{F}}_{i,l}^{y=W} \cosh \bar{\nu}_l y - \bar{\tilde{F}}_{i,l}^{y=0} \cosh \bar{\nu}_l (W-y) \right) \frac{\sin \kappa_l z}{\bar{\nu}_l \sinh \bar{\nu}_l W}, \ i = x \text{ or } z. \tag{69}$$

Considering the boundary conditions, $\bar{H}_{y1}$ must have the same form as $\bar{H}_{x2}$ and $\bar{H}_{z2}$, and $\bar{H}_{y2}$ must have the same form as $\bar{H}_{x1}$ and $\bar{H}_{z1}$. Hence,

$$\bar{H}_{y1}(x,y,z) = e^{-jkx} \sum_{n=1}^{\infty} \left(\bar{\tilde{F}}_{y,n}^{z=T} \cosh \bar{\eta}_n z - \bar{\tilde{F}}_{y,n}^{z=0} \cosh \bar{\eta}_n (T-z) \right) \frac{\sin K_n y}{\bar{\eta}_n \sinh \bar{\eta}_n T}, \tag{70}$$

$$\bar{H}_{y2}(x,y,z) = e^{-jkx} \sum_{l=0}^{\infty} \left(\bar{\tilde{f}}_{y,\mathrm{c},l}^{y=0} \sinh \bar{\nu}_l (W-y) + \bar{\tilde{f}}_{y,\mathrm{c},l}^{y=W} \sinh \bar{\nu}_l y \right) \frac{\cos \kappa_l z}{\sinh \bar{\nu}_l W}. \tag{71}$$

Equations (5), (65), (69), (70) and (71) give that $\bar{\mathbf{E}}$ contributions can be written as

$$\begin{aligned}
\bar{E}_{x\eta}(x,y,z) &= -\frac{e^{-jkx}}{\sigma + j\omega\varepsilon} \sum_{n=1}^{\infty} \frac{\sin K_n y}{\sinh \bar{\eta}_n T} \cdot \Big[\left(\bar{\tilde{f}}_{z,\mathrm{c},n}^{z=0} \sinh \bar{\eta}_n (T-z) + \bar{\tilde{f}}_{z,\mathrm{c},n}^{z=T} \sinh \bar{\eta}_n z \right) K_n \\
&\quad + \bar{\tilde{F}}_{y,n}^{z=T} \sinh \bar{\eta}_n z + \bar{\tilde{F}}_{y,n}^{z=0} \sinh \bar{\eta}_n (T-z) \Big], \qquad (72) \\
\bar{E}_{x\nu}(x,y,z) &= \frac{e^{-jkx}}{\sigma + j\omega\varepsilon} \sum_{l=1}^{\infty} \frac{\sin \kappa_l z}{\sinh \bar{\nu}_l W} \cdot \Big[\left(\bar{\tilde{F}}_{z,l}^{y=W} \sinh \bar{\nu}_l y + \bar{\tilde{F}}_{z,l}^{y=0} \sinh \bar{\nu}_l (W-y) \right) \\
&\quad + \left(\bar{\tilde{f}}_{y,\mathrm{c},l}^{y=0} \sinh \bar{\nu}_l (W-y) + \bar{\tilde{f}}_{y,\mathrm{c},l}^{y=W} \sinh \bar{\nu}_l y \right) \kappa_l \Big], \qquad (73) \\
\bar{E}_{y\eta}(x,y,z) &= \frac{e^{-jkx}}{\sigma + j\omega\varepsilon} \sum_{n=0}^{\infty} \frac{\cos K_n y}{\sinh \bar{\eta}_n T} \cdot \Big[\bar{\eta}_n \left(\bar{\tilde{f}}_{x,\mathrm{c},n}^{z=T} \cosh \bar{\eta}_n z - \bar{\tilde{f}}_{x,\mathrm{c},n}^{z=0} \cosh \bar{\eta}_n (T-z) \right) \\
&\quad + jk \left(\bar{\tilde{f}}_{z,\mathrm{c},n}^{z=0} \sinh \bar{\eta}_n (T-z) + \bar{\tilde{f}}_{z,\mathrm{c},n}^{z=T} \sinh \bar{\eta}_n z \right) \Big], \qquad (74) \\
\bar{E}_{y\nu}(x,y,z) &= \frac{e^{-jkx}}{\sigma + j\omega\varepsilon} \sum_{l=1}^{\infty} \frac{1}{\bar{\nu}_l \sinh \bar{\nu}_l W} \cdot \Big[\left(\bar{\tilde{F}}_{x,l}^{y=W} \cosh \bar{\nu}_l y - \bar{\tilde{F}}_{x,l}^{y=0} \cosh \bar{\nu}_l (W-y) \right) \kappa_l \cos \kappa_l z \\
&\quad + jk \left(\bar{\tilde{F}}_{z,l}^{y=W} \cosh \bar{\nu}_l y - \bar{\tilde{F}}_{z,l}^{y=0} \cosh \bar{\nu}_l (W-y) \right) \sin \kappa_l z \Big], \qquad (75) \\
\bar{E}_{z\eta}(x,y,z) &= \frac{e^{-jkx}}{\sigma + j\omega\varepsilon} \sum_{n=1}^{\infty} \frac{\sin K_n y}{\sinh \bar{\eta}_n T} \cdot \Big[\frac{jk}{\bar{\eta}_n} \left(\bar{\tilde{F}}_{y,n}^{z=0} \cosh \bar{\eta}_n (T-z) - \bar{\tilde{F}}_{y,n}^{z=T} \cosh \bar{\eta}_n z \right) \\
&\quad + \left(\bar{\tilde{f}}_{x,\mathrm{c},n}^{z=0} \sinh \bar{\eta}_n (T-z) + \bar{\tilde{f}}_{x,\mathrm{c},n}^{z=T} \sinh \bar{\eta}_n z \right) K_n \Big], \qquad (76) \\
\bar{E}_{z\nu}(x,y,z) &= \frac{e^{-jkx}}{\sigma + j\omega\varepsilon} \sum_{l=0}^{\infty} \frac{-1}{\sinh \bar{\nu}_l W} \cdot \Big[jk \left(\bar{\tilde{f}}_{y,\mathrm{c},l}^{y=0} \sinh \bar{\nu}_l (W-y) + \bar{\tilde{f}}_{y,\mathrm{c},l}^{y=W} \sinh \bar{\nu}_l y \right) \cos \kappa_l z \\
&\quad + \left(\bar{\tilde{F}}_{x,l}^{y=W} \sinh \bar{\nu}_l y + \bar{\tilde{F}}_{x,l}^{y=0} \sinh \bar{\nu}_l (W-y) \right) \sin \kappa_l z \Big]. \qquad (77)
\end{aligned}$$

Because of the orthogonality of the eigenfunctions from the same eigenfunction system, each of the continuity equations (53) to (56) implies a continuity condition for each mode with a y dependent eigenfunction. The procedure to get a continuity condition for each mode n of a field component is to multiply the continuity equation for the field component by the eigenfunction of the mode and then

integrate the continuity equation for the field component from $y = 0$ to W. In that way, Eq. (65) with $i = x$ inserted in Eq. (53) gives

$$\bar{\tilde{f}}^{z_e=T_e}_{ex,\mathrm{c},n} = \bar{\tilde{f}}^{z_s=0}_{sx,\mathrm{c},n}, n = 0, 1, 2, \ldots. \tag{78}$$

Similarly, Eqs. (70) and (71) inserted in Eq. (53) give

$$\frac{W}{2}\frac{\bar{\tilde{F}}^{z_e=T_e}_{ey,n}\cosh\bar{\eta}_{e,n}T_e - \bar{\tilde{F}}^{z_e=0}_{ey,n}}{\bar{\eta}_{e,n}\sinh\bar{\eta}_{e,n}T_e} + \bar{I}_{ey,n} = \frac{W}{2}\frac{\bar{\tilde{F}}^{z_s=T_s}_{sy,n} - \bar{\tilde{F}}^{z_s=0}_{sy,n}\cosh\bar{\eta}_{s,n}T_s}{\bar{\eta}_{s,n}\sinh\bar{\eta}_{s,n}T_s} + \bar{I}_{sy,n} \tag{79}$$

where $n = 1, 2, 3, \ldots$, and

$$\bar{I}_{ey,n} = \int_0^W \sum_{l=0}^{\infty}\left(\bar{\tilde{f}}^{y=0}_{ey,\mathrm{c},l}\sinh\bar{\nu}_{e,l}(W-y) + \bar{\tilde{f}}^{y=W}_{ey,\mathrm{c},l}\sinh\bar{\nu}_{e,l}y\right)\frac{(-1)^l}{\sinh\bar{\nu}_{e,l}W}\sin K_n y\mathrm{d}y, \tag{80}$$

$$\bar{I}_{sy,n} = \int_0^W \sum_{l=0}^{\infty}\left(\bar{\tilde{f}}^{y=0}_{sy,\mathrm{c},l}\sinh\bar{\nu}_{s,l}(W-y) + \bar{\tilde{f}}^{y=W}_{sy,\mathrm{c},l}\sinh\bar{\nu}_{s,l}y\right)\frac{1}{\sinh\bar{\nu}_{s,l}W}\sin K_n y\mathrm{d}y. \tag{81}$$

Equation (65) with $i = z$ inserted in Eq. (54) gives

$$\mu_e\bar{\tilde{f}}^{z_e=T_e}_{ez,\mathrm{c},n} = \mu_s\bar{\tilde{f}}^{z_s=0}_{sz,\mathrm{c},n}, n = 0, 1, 2, \ldots. \tag{82}$$

Insertion of Eqs. (72) and (73) into Eq. (56) gives

$$\frac{\bar{F}^{z_e=T_e}_{ey,n} + K_n\bar{f}^{z_e=T_e}_{ez,\mathrm{c},n}}{\bar{\sigma}_e} = \frac{\bar{F}^{z_s=0}_{sy,n} + K_n\bar{f}^{z_s=0}_{sz,\mathrm{c},n}}{\bar{\sigma}_s}, \quad n = 1, 2, 3, \ldots. \tag{83}$$

Insertion of Eqs. (74) and (75) into Eq. (56) gives

$$\begin{aligned}&\frac{(1+\delta_{n,0})W}{2\bar{\sigma}_e\sinh\bar{\eta}_{e,n}T_e}\left[\bar{\eta}_{e,n}\left(\bar{\tilde{f}}^{z_e=T_e}_{ex,\mathrm{c},n}\cosh\bar{\eta}_{e,n}T_e - \bar{\tilde{f}}^{z_e=0}_{ex,\mathrm{c},n}\right) + jk\bar{\tilde{f}}^{z_e=T_e}_{ez,\mathrm{c},n}\sinh\bar{\eta}_{e,n}T_e\right] + \frac{\bar{I}_{ex,n}}{\bar{\sigma}_e}\\ =\ &\frac{(1+\delta_{n,0})W}{2\bar{\sigma}_s\sinh\bar{\eta}_{s,n}T_s}\left[\bar{\eta}_{s,n}\left(\bar{\tilde{f}}^{z_s=T_s}_{sx,\mathrm{c},n} - \bar{\tilde{f}}^{z_s=0}_{sx,\mathrm{c},n}\cosh\bar{\eta}_{s,n}T_s\right) + jk\bar{\tilde{f}}^{z_s=0}_{sz,\mathrm{c},n}\sinh\bar{\eta}_{s,n}T_s\right] + \frac{\bar{I}_{sx,n}}{\bar{\sigma}_s}, n = 0, 1, 2, \ldots\end{aligned} \tag{84}$$

where $\delta_{n,0} = 1$ if $n = 0$, $\delta_{n,0} = 0$ if $n \neq 0$, and

$$\bar{I}_{ex,n} = \int_0^W \sum_{l=1}^{\infty}\left(\bar{\tilde{F}}^{y=W}_{ex,l}\cosh\bar{\nu}_{e,l}y - \bar{\tilde{F}}^{y=0}_{ex,l}\cosh\bar{\nu}_{e,l}(W-y)\right)\frac{(-1)^l\kappa_{e,l}\cos K_n y\mathrm{d}y}{\bar{\nu}_{e,l}\sinh\bar{\nu}_{e,l}W}, \tag{85}$$

$$\bar{I}_{sx,n} = \int_0^W \sum_{l=1}^{\infty}\left(\bar{\tilde{F}}^{y=W}_{sx,l}\cosh\bar{\nu}_{s,l}y - \bar{\tilde{F}}^{y=0}_{sx,l}\cosh\bar{\nu}_{s,l}(W-y)\right)\frac{\kappa_{s,l}\cos K_n y\mathrm{d}y}{\bar{\nu}_{s,l}\sinh\bar{\nu}_{s,l}W}. \tag{86}$$

Strictly, $\kappa_{e,l}$ and $\kappa_{s,l}$ depend on the slice thickness, not the material, but with one slice thickness per material, the subscripts should not be confusing. With $i = z$, Eqs. (65) and (69) inserted in Eq. (55) give

$$\begin{aligned}&\frac{(1+\delta_{n,0})W\bar{\eta}_{e,n}}{2\sinh\bar{\eta}_{e,n}T_e}\left(\bar{\tilde{f}}^{z_e=T_e}_{ez,\mathrm{c},n}\cosh\bar{\eta}_{e,n}T_e - \bar{\tilde{f}}^{z_e=0}_{ez,\mathrm{c},n}\right) + \bar{I}_{ez,n}\\ =\ &\frac{(1+\delta_{n,0})W\bar{\eta}_{s,n}}{2\sinh\bar{\eta}_{s,n}T_s}\left(\bar{\tilde{f}}^{z_s=T_s}_{sz,\mathrm{c},n} - \bar{\tilde{f}}^{z_s=0}_{sz,\mathrm{c},n}\cosh\bar{\eta}_{s,n}T_s\right) + \bar{I}_{sz,n}\end{aligned} \tag{87}$$

where $n = 0, 1, 2, \ldots$, and

$$\bar{I}_{ez,n} = \int_0^W \sum_{l=1}^{\infty}\left(\bar{\tilde{F}}^{y=W}_{ez,l}\cosh\bar{\nu}_{e,l}y - \bar{\tilde{F}}^{y=0}_{ez,l}\cosh\bar{\nu}_{e,l}(W-y)\right)\frac{(-1)^l\kappa_{e,l}\cos K_n y\mathrm{d}y}{\bar{\nu}_{e,l}\sinh\bar{\nu}_{e,l}W}, \tag{88}$$

$$\bar{I}_{sz,n} = \int_0^W \sum_{l=1}^{\infty}\left(\bar{\tilde{F}}^{y=W}_{sz,l}\cosh\bar{\nu}_{s,l}y - \bar{\tilde{F}}^{y=0}_{sz,l}\cosh\bar{\nu}_{s,l}(W-y)\right)\frac{\kappa_{s,l}\cos K_n y\mathrm{d}y}{\bar{\nu}_{s,l}\sinh\bar{\nu}_{s,l}W}. \tag{89}$$

The integrals given by Eqs. (80), (81), (85), (86), (88) and (89) are here referred to as *interface integrals*. Equations (78), (79), (82), (83), (84) and (87) are linear equations that completely determine the unknown Fourier coefficients for modes with number n, each corresponding to a y dependent sine or cosine eigenfunction. Equations (82) and (87) give

$$\bar{\tilde{f}}^{z_s=0}_{sz,\mathrm{c},n} = \frac{\bar{\Gamma}_{e,n}\bar{\tilde{f}}^{z_e=0}_{ez,\mathrm{c},n} + \bar{\Gamma}_{s,n}\bar{\tilde{f}}^{z_s=T_s}_{sz,\mathrm{c},n} + \bar{I}_{sz,n} - \bar{I}_{ez,n}}{\frac{\mu_s}{\mu_e}\bar{\Lambda}_{e,n} + \bar{\Lambda}_{s,n}} \tag{90}$$

where $n = 0, 1, 2, \ldots$, and

$$\bar{\Gamma}_{i,n} = \frac{(1+\delta_{n,0})W\bar{\eta}_{i,n}}{2\sinh\bar{\eta}_{i,n}T_i}, \qquad \bar{\Lambda}_{i,n} = \frac{(1+\delta_{n,0})W\bar{\eta}_{i,n}}{2\tanh\bar{\eta}_{i,n}T_i},\ i = e \text{ or } s. \tag{91}$$

Since all parameters on the right hand side of Eq. (90) are known, Eq. (90) determines $\bar{\tilde{f}}^{z_s=0}_{sz,\mathrm{c},n}$ fully. Combined with Eqs. (82) and (90), $\bar{\tilde{f}}^{z_e=T_e}_{ez,\mathrm{c},n}$ is also determined. Equations (58), (78), (82) and (91) inserted in Eq. (84) give

$$\bar{\tilde{f}}^{z_s=0}_{sx,\mathrm{c},n} = \frac{1}{\bar{R}_{e,n}+\bar{R}_{s,n}}\left[\bar{G}_{e,n}\bar{\tilde{f}}^{z_e=0}_{ex,\mathrm{c},n} + \bar{G}_{s,n}\bar{\tilde{f}}^{z_s=T_s}_{sx,\mathrm{c},n} + \left(\bar{O}_{s,n} - \bar{O}_{e,n}\frac{\mu_s}{\mu_e}\right)\bar{\tilde{f}}^{z_s=0}_{sz,\mathrm{c},n} + \frac{\bar{I}_{sx,n}}{\bar{\sigma}_s} - \frac{\bar{I}_{ex,n}}{\bar{\sigma}_e}\right] \tag{92}$$

where $n = 0, 1, 2, \ldots$, and

$$\bar{G}_{i,n} = \frac{\bar{\Gamma}_{i,n}}{\bar{\sigma}_i}, \qquad \bar{R}_{i,n} = \frac{\bar{\Lambda}_{i,n}}{\bar{\sigma}_i}, \qquad \bar{O}_{i,n} = jk\frac{(1+\delta_{n,0})W}{2\bar{\sigma}_i},\ i = e \text{ or } s. \tag{93}$$

which with Eq. (90) makes $\bar{\tilde{f}}^{z_s=0}_{sx,\mathrm{c},n}$ fully determined. Because of Eq. (78), Eq. (92) also gives $\bar{\tilde{f}}^{z_e=T_e}_{ex,\mathrm{c},n}$. Equations (82) and (58) inserted in Eq. (83) give

$$\bar{\tilde{F}}^{z_s=0}_{sy,n} = \bar{q}\bar{\tilde{F}}^{z_e=T_e}_{ey,n} + \left(\bar{q}\frac{\mu_s}{\mu_e} - 1\right)K_n\bar{\tilde{f}}^{z_s=0}_{sz,\mathrm{c},n}, \quad n = 1, 2, 3, \ldots. \tag{94}$$

Equation (94) inserted in Eq. (79) gives

$$\bar{\tilde{F}}^{z_e=T_e}_{ey,n} = \frac{1}{\bar{C}_{e,n}+\bar{q}\bar{C}_{s,n}}\left(\bar{S}_{e,n}\bar{\tilde{F}}^{z_e=0}_{ey,n} + \bar{S}_{s,n}\bar{\tilde{F}}^{z_s=T_s}_{sy,n} + \bar{C}_{s,n}\left(1-\bar{q}\frac{\mu_s}{\mu_e}\right)K_n\bar{\tilde{f}}^{z_s=0}_{sz,\mathrm{c},n} + \bar{I}_{sy,n} - \bar{I}_{ey,n}\right) \tag{95}$$

where $n = 1, 2, 3, \ldots$, and

$$\bar{S}_{i,n} = \frac{W}{2\bar{\eta}_{i,n}\sinh\bar{\eta}_{i,n}T_i}, \qquad \bar{C}_{i,n} = \frac{W}{2\bar{\eta}_{i,n}\tanh\bar{\eta}_{i,n}T_i},\ i = e \text{ or } s. \tag{96}$$

Finally, Eqs. (95) and (90) in Eq. (94) fully determine $\bar{\tilde{F}}^{z_s=0}_{sy,n}$ for $n = 1, 2, 3, \ldots$. From the solutions above, it can be concluded that the boundary conditions on a material interface depend partly on the boundary conditions on the laminate at $y = 0$ and W via interface integrals. In numerical examples mentioned in Section 3, the interface integrals are significant and, for $\bar{H}_z$, dominate the contributions to the Fourier coefficients of the internal boundary functions. The large influence of $\bar{I}_{ez}$ and $\bar{I}_{sz}$ on $\bar{H}_z$ is caused by a rapid change of $\bar{H}_z$ with y at $y = 0$ and W. It should be noted that the continuity Equations (79) and (83) are only needed for determination of $\bar{\tilde{F}}^{z_e=T_e}_{ey,n}$ and $\bar{\tilde{F}}^{z_s=0}_{sy,n}$ and do not exist for $n = 0$.

2.2.1. Determination of Neumann Boundary Functions

The use of Neumann conditions instead of Dirichlet conditions requires more calculation steps, but not necessarily more measurements if boundary conditions are measured. The Neumann boundary Fourier coefficients in Eqs. (69) and (70) are needed. Fortunately, direct measurement of the normal derivatives of $\bar{\mathbf{H}}$ in the laminate is not necessary. Because of the continuity condition on the normal component of $\bar{\mathbf{B}}$, Ampère's law and continuity conditions on tangential $\bar{\mathbf{E}}$ components, it is sufficient to measure some $\bar{\mathbf{H}}$ components and certain tangential $\bar{\mathbf{E}}$ components on the laminate surface, and then calculate the

needed normal derivatives within the laminate materials. From known $\bar{\mathbf{H}}$ on a boundary it is possible to calculate tangential derivatives of $\bar{\mathbf{H}}$ but not the normal derivative of a tangential $\bar{\mathbf{H}}$ component since the dependence of $\bar{\mathbf{H}}$ on the coordinate of the normal direction is not given by the boundary values of $\bar{\mathbf{H}}$. Furthermore, it is sufficient to do the measurements along lines at some constant x coordinate. The continuity condition of $\bar{H}_y$ at plane boundaries with constant y between an ambient material, a, and an arbitrary material, s, in the laminate is

$$\bar{H}_{sy} = \frac{\mu_a}{\mu_s}\bar{H}_{ay}. \tag{97}$$

For the boundary surfaces at constant y, the z component of Ampère's law in material s combined with Eq. (97) gives

$$\frac{\partial \bar{H}_{sx}(x,0,z)}{\partial y} = \frac{\mu_a}{\mu_s}\frac{\partial \bar{H}_{ay}(x,0,z)}{\partial x} - (\sigma_s + j\omega\varepsilon_s)\bar{E}_z(x,0,z), \tag{98}$$

$$\frac{\partial \bar{H}_{sx}(x,W,z)}{\partial y} = \frac{\mu_a}{\mu_s}\frac{\partial \bar{H}_{ay}(x,W,z)}{\partial x} - (\sigma_s + j\omega\varepsilon_s)\bar{E}_z(x,W,z) \tag{99}$$

where material indicator subscript has been skipped for $\bar{E}_z$ since $\bar{E}_z$ is a tangential component at constant y and therefore continuous there. According to Eq. (66), $\frac{\partial \bar{H}_x(x,0,z)}{\partial y}$ and $\frac{\partial \bar{H}_x(x,W,z)}{\partial y}$ are Fourier series expressed with $\sin\kappa_l z$ eigenfunctions. It is appropriate to express also the functions on the right hand sides of Eqs. (98) and (99) as Fourier series of $\sin\kappa_{s,l} z$. Then the orthogonality of these eigenfunctions can be used to determine Fourier coefficients in the Neumann boundary functions in Eq. (66). Fourier series of $\bar{H}_y(x,0,z)$ and $\bar{H}_y(x,W,z)$ expressed with $\sin\kappa_{s,l} z$ functions are needed for the sole purpose of determining Fourier coefficients in Neumann boundary functions. The additional Fourier series required are given by Eq. (30) with $i = y$. This gives

$$\frac{\partial \bar{H}_{ay}(x,0,z)}{\partial x} = -jke^{-jkx}\sum_{l=1}^{\infty}\bar{\bar{f}}_{ay,l}^{y=0}\sin\kappa_{s,l}z, \quad \frac{\partial \bar{H}_{ay}(x,W,z)}{\partial x} = -jke^{-jkx}\sum_{l=1}^{\infty}\bar{\bar{f}}_{ay,l}^{y=W}\sin\kappa_{s,l}z. \tag{100}$$

The Fourier series of $\bar{E}_i(x,0,z)$ and $\bar{E}_i(x,W,z)$ can be obtained from Eq. (44). These Fourier series and Eq. (100) inserted in Eqs. (98) and (99) multiplied by $\sin\kappa_{s,l}z$ and then integrated from $z = 0$ to T_s give the Fourier coefficients of the Neumann boundary functions with $i = x$ in Eq. (69) in the laminate material s. The coefficients are

$$\bar{\bar{F}}_{sx,l}^{y=0} = -jk\frac{\mu_a}{\mu_s}\bar{\bar{f}}_{ay,l}^{y=0} - (\sigma_s + j\omega\varepsilon_s)\bar{\bar{g}}_{z,l}^{y=0}, \quad \bar{\bar{F}}_{sx,l}^{y=W} = -jk\frac{\mu_a}{\mu_s}\bar{\bar{f}}_{ay,l}^{y=W} - (\sigma_s + j\omega\varepsilon_s)\bar{\bar{g}}_{z,l}^{y=W}. \tag{101}$$

The other Fourier coefficients in Eqs. (69) and (70) are determined similarly and are given by

$$\bar{\bar{F}}_{sz,l}^{y=0} = -\kappa_{s,l}\frac{\mu_a}{\mu_s}\bar{\bar{f}}_{ay,\mathrm{c},l}^{y=0} + (\sigma_s + j\omega\varepsilon_s)\bar{\bar{g}}_{x,l}^{y=0}, \quad \bar{\bar{F}}_{sz,l}^{y=W} = -\kappa_{s,l}\frac{\mu_a}{\mu_s}\bar{\bar{f}}_{ay,\mathrm{c},l}^{y=W} + (\sigma_s + j\omega\varepsilon_s)\bar{\bar{g}}_{x,l}^{y=W}, \tag{102}$$

$$\bar{\bar{F}}_{sy,n}^{z=0} = -K_n\frac{\mu_a}{\mu_s}\bar{\bar{f}}_{az,\mathrm{c},n}^{z=0} - (\sigma_s + j\omega\varepsilon_s)\bar{\bar{g}}_{x,n}^{z=0}, \quad \bar{\bar{F}}_{sy,n}^{z=T} = -K_n\frac{\mu_a}{\mu_s}\bar{\bar{f}}_{az,\mathrm{c},n}^{z=T} - (\sigma_s + j\omega\varepsilon_s)\bar{\bar{g}}_{x,n}^{z=T}. \tag{103}$$

In FE results, all field values can be taken from material s. In that case, Eqs. (101), (102) and (103) are valid with subscript a replaced by subscript s.

2.3. A Laminate with an Arbitrary Number of Rectangular, Infinitely Long, Isotropic Plates

The material layers and interfaces are numbered from one end to the other according to Fig. 3.

With interface number as a superscript, material number as a subscript, and mode subscript n skipped for compactness everywhere, including the eigenvalue K_n, some parameters that make the equations more compact are

$$\bar{\sigma}_i \equiv \sigma_i + j\omega\varepsilon_i, \quad \bar{q}^i \equiv \frac{\bar{\sigma}_{i+1}}{\bar{\sigma}_i}, \quad M^i \equiv \frac{\mu_i}{\mu_{i+1}}, \tag{104}$$

$$\bar{D}_x^i \equiv \frac{\bar{I}_{i+1,x}^i}{\bar{\sigma}_{i+1}} - \frac{\bar{I}_{i,x}^i}{\bar{\sigma}_i}, \quad \bar{D}_y^i \equiv \bar{I}_{i+1,y}^i - \bar{I}_{i,y}^i, \quad \bar{D}_z^i \equiv \bar{I}_{i+1,z}^i - \bar{I}_{i,z}^i \tag{105}$$

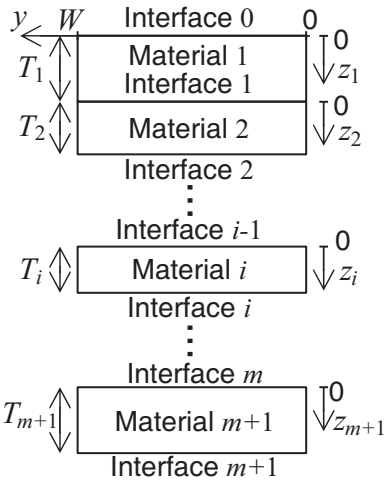

Figure 3. Cross section of a laminate with $m+1$ material layers.

where $\bar{I}^i_{i,x}$, $\bar{I}^i_{i+1,x}$, $\bar{I}^i_{i,y}$, $\bar{I}^i_{i+1,y}$, $\bar{I}^i_{i,z}$ and $\bar{I}^i_{i+1,z}$ are given by Eqs. (85), (86), (80), (81), (88) and (89), respectively, with $e = i$ and $s = i+1$. The six linear continuity equations per material interface and mode n, Eqs. (78), (79), (82), (83), (84) and (87), can be written as

$$\bar{\bar{f}}^i_{i,x} = \bar{\bar{f}}^i_{i+1,x},\ n = 0,1,2,\ldots, \tag{106}$$

$$\bar{C}_i\bar{\bar{F}}^i_{i,y} - \bar{S}_i\bar{\bar{F}}^{i-1}_{i,y} = \bar{S}_{i+1}\bar{\bar{F}}^{i+1}_{i+1,y} - \bar{C}_{i+1}\bar{\bar{F}}^i_{i+1,y} + \bar{D}^i_y,\ n = 1,2,3,\ldots, \tag{107}$$

$$\bar{\bar{f}}^i_{i+1,z} = M^i\bar{\bar{f}}^i_{i,z},\ n = 0,1,2,\ldots, \tag{108}$$

$$\bar{\bar{F}}^i_{i+1,y} = \bar{q}^i\bar{\bar{F}}^i_{i,y} + K\left(\bar{q}^i\bar{\bar{f}}^i_{i,z} - \bar{\bar{f}}^i_{i+1,z}\right),\ n = 1,2,3,\ldots, \tag{109}$$

$$\bar{R}_i\bar{\bar{f}}^i_{i,x} - \bar{G}_i\bar{\bar{f}}^{i-1}_{i,x} + \bar{O}_i\bar{\bar{f}}^i_{i,z} = \bar{G}_{i+1}\bar{\bar{f}}^{i+1}_{i+1,x} - \bar{R}_{i+1}\bar{\bar{f}}^i_{i+1,x} + \bar{O}_{i+1}\bar{\bar{f}}^i_{i+1,z} + \bar{D}^i_x,\ n = 0,1,2,\ldots, \tag{110}$$

$$\bar{\Lambda}_i\bar{\bar{f}}^i_{i,z} - \bar{\Gamma}_i\bar{\bar{f}}^{i-1}_{i,z} = \bar{\Gamma}_{i+1}\bar{\bar{f}}^{i+1}_{i+1,z} - \bar{\Lambda}_{i+1}\bar{\bar{f}}^i_{i+1,z} + \bar{D}^i_z,\ n = 0,1,2,\ldots. \tag{111}$$

For mode $n = 0$, there are only four continuity equations per internal material interface since the sine eigenfunctions in the Fourier series in Eqs. (70) and (72), and consequently Eqs. (107) and (109), do not have this mode. For each mode, the continuity equations (106), (108), (110) and (111) evaluated for all internal material interfaces can be combined to an equation system that can be solved, with respect to the unknown Fourier coefficients with subscripts x and z, independently of the the other continuity equations. The latter determine unknown Fourier coefficients with subscript y and can be solved after, but not before, the Fourier coefficients with subscripts x and z have been determined. The sizes of the equation systems can be reduced if the unknown Fourier coefficients of either the higher or the lower numbered material at each internal interface are eliminated from Equations (107), (110) and (111) by use of Eqs. (106), (108) and (109), before the equation systems of first Eqs. (110) and (111), and later, Eq. (107), are solved. After that is done, Eqs. (106), (108) and (109) can be reused to calculate the previously eliminated Fourier coefficients. Three main cases can be distinguished for each continuity equation depending on which Fourier coefficients are known. The first case has only one internal material interface. The second case has two interfaces. The third case has more than two interfaces. Below, each continuity equation is arranged with only known terms on the right hand side, which is convenient for subsequent matrix formulation. Each of the following equations involves more than one interface and is referred to by the interface number of the $\bar{D}$ term. For interface 1 when $m > 1$, Eqs. (106) and (108) inserted in Eq. (110) give

$$\left(\bar{R}_1 + \bar{R}_2\right)\bar{\bar{f}}^1_{1,x} + \left(\bar{O}_1 - \bar{O}_2M^1\right)\bar{\bar{f}}^1_{1,z} - \bar{G}_2\bar{\bar{f}}^2_{2,x} = \bar{G}_1\bar{\bar{f}}^0_{1,x} + \bar{D}^1_x,\quad n = 0,1,2,\ldots. \tag{112}$$

For interface 1 when $m > 1$, Eq. (108) inserted in Eq. (111) gives

$$\left(\bar{\Lambda}_1 + \bar{\Lambda}_2M^1\right)\bar{\bar{f}}^1_{1,z} - \bar{\Gamma}_2\bar{\bar{f}}^2_{2,z} = \bar{\Gamma}_1\bar{\bar{f}}^0_{1,z} + \bar{D}^1_z,\quad n = 0,1,2,\ldots. \tag{113}$$

Equations (112) and (113) are valid also when $m = 1$, but then the terms $\bar{G}_2\bar{\bar{f}}^2_{2,x}$ and $\bar{\Gamma}_2\bar{\bar{f}}^2_{2,z}$ are known and should be on the right hand side of Eqs. (112) and (113), respectively. For interface $i \in [2, m-1]$ when $m > 2$, Eqs. (106) and (108) inserted in Eq. (110) give

$$-\bar{G}_i\bar{\bar{f}}^{i-1}_{i-1,x} + \left(\bar{R}_i + \bar{R}_{i+1}\right)\bar{\bar{f}}^i_{i,x} + \left(\bar{O}_i - \bar{O}_{i+1}M^i\right)\bar{\bar{f}}^i_{i,z} - \bar{G}_{i+1}\bar{\bar{f}}^{i+1}_{i+1,x} = \bar{D}^i_x, \quad n = 0, 1, 2, \ldots. \tag{114}$$

For interface $i \in [2, m-1]$ when $m > 2$, Eq. (108) inserted in Eq. (111) gives

$$-\bar{\Gamma}_i M^{i-1}\bar{\bar{f}}^{i-1}_{i-1,z} + \left(\bar{\Lambda}_i + \bar{\Lambda}_{i+1}M^i\right)\bar{\bar{f}}^i_{i,z} - \bar{\Gamma}_{i+1}\bar{\bar{f}}^{i+1}_{i+1,z} = \bar{D}^i_z, \quad n = 0, 1, 2, \ldots. \tag{115}$$

For interface m when $m > 1$, Eqs. (106) and (108) inserted in Eq. (110) give

$$-\bar{G}_m\bar{\bar{f}}^{m-1}_{m-1,x} + \left(\bar{R}_m + \bar{R}_{m+1}\right)\bar{\bar{f}}^m_{m,x} + \left(\bar{O}_m - \bar{O}_{m+1}M^m\right)\bar{\bar{f}}^m_{m,z} = \bar{G}_{m+1}\bar{\bar{f}}^{m+1}_{m+1,x} + \bar{D}^m_x, \; n = 0, 1, 2, \ldots. \tag{116}$$

For interface m when $m > 1$, Eq. (108) inserted in Eq. (111) gives

$$-\bar{\Gamma}_m M^{m-1}\bar{\bar{f}}^{m-1}_{m-1,z} + \left(\bar{\Lambda}_m + \bar{\Lambda}_{m+1}M^m\right)\bar{\bar{f}}^m_{m,z} = \bar{\Gamma}_{m+1}\bar{\bar{f}}^{m+1}_{m+1,z} + \bar{D}^m_z, \quad n = 0, 1, 2, \ldots. \tag{117}$$

For each mode n, the linear equation system of Eqs. (110) and (111) for m internal material interfaces can be written as

$$\bar{\mathbf{A}}\bar{\bar{\mathbf{f}}}_{\mathbf{x,z}} = \bar{\mathbf{h}}_{\mathbf{x,z}} \tag{118}$$

where $\bar{\mathbf{A}}$ is a matrix with $2m \times 2m$ elements that can be identified with the coefficients on the left hand sides of Eqs. (112)–(117), $\bar{\bar{\mathbf{f}}}_{\mathbf{x,z}}$ is a vector with $2m$ elements containing the lower material numbered Fourier coefficients with subscripts x and z for each internal material interface, and $\bar{\mathbf{h}}_{x,z}$ is a vector with $2m$ elements containing the known right hand sides of Eqs. (112)–(117). The block tridiagonal structure of $\bar{\mathbf{A}}$ can be illustrated by the case of $m = 4$. In this case, Eq. (118) can be written as

$$\left[\begin{array}{cc|cc|cc|cc}
\bar{a}_{11} & \bar{a}_{12} & \bar{a}_{13} & 0 & 0 & 0 & 0 & 0 \\
0 & \bar{a}_{22} & 0 & \bar{a}_{24} & 0 & 0 & 0 & 0 \\
\hline
\bar{a}_{31} & 0 & \bar{a}_{33} & \bar{a}_{34} & \bar{a}_{35} & 0 & 0 & 0 \\
0 & \bar{a}_{42} & 0 & \bar{a}_{44} & 0 & \bar{a}_{46} & 0 & 0 \\
\hline
0 & 0 & \bar{a}_{53} & 0 & \bar{a}_{55} & \bar{a}_{56} & \bar{a}_{57} & 0 \\
0 & 0 & 0 & \bar{a}_{64} & 0 & \bar{a}_{66} & 0 & \bar{a}_{68} \\
\hline
0 & 0 & 0 & 0 & \bar{a}_{75} & 0 & \bar{a}_{77} & \bar{a}_{78} \\
0 & 0 & 0 & 0 & 0 & \bar{a}_{86} & 0 & \bar{a}_{88}
\end{array}\right]
\left[\begin{array}{c}
\bar{\bar{f}}^1_{1,x} \\ \bar{\bar{f}}^1_{1,z} \\ \hline \bar{\bar{f}}^2_{2,x} \\ \bar{\bar{f}}^2_{2,z} \\ \hline \bar{\bar{f}}^3_{3,x} \\ \bar{\bar{f}}^3_{3,z} \\ \hline \bar{\bar{f}}^4_{4,x} \\ \bar{\bar{f}}^4_{4,z}
\end{array}\right] =
\left[\begin{array}{c}
\bar{h}^1_x \\ \bar{h}^1_z \\ \hline \bar{h}^2_x \\ \bar{h}^2_z \\ \hline \bar{h}^3_x \\ \bar{h}^3_z \\ \hline \bar{h}^4_x \\ \bar{h}^4_z
\end{array}\right] \tag{119}$$

For interface 1 when $m > 1$, Eqs. (108) and (109) inserted in Eq. (107) give

$$\left(\bar{C}_1 + \bar{C}_2\bar{q}^1\right)\bar{\bar{F}}^1_{1,y} - \bar{S}_2\bar{\bar{F}}^2_{2,y} = \bar{C}_2K\left(M^1 - \bar{q}^1\right)\bar{\bar{f}}^1_{1,z} + \bar{S}_1\bar{\bar{F}}^0_{1,y} + \bar{D}^1_y, \quad n = 1, 2, 3, \ldots \tag{120}$$

where $\bar{\bar{F}}^0_{1,y}$ can be calculated from the ambient material according to Eq. (103). Equation (120) is valid also when $m = 1$, but then the term $\bar{S}_2\bar{\bar{F}}^2_{2,y}$ is known and should be on the right hand side of Eq. (120). For interface $i \in [2, m-1]$ when $m > 2$, Eqs. (108) and (109) inserted in Eq. (107) give

$$\begin{aligned}
&-\bar{S}_i\bar{q}^{i-1}\bar{\bar{F}}^{i-1}_{i-1,y} + \left(\bar{C}_i + \bar{C}_{i+1}\bar{q}^i\right)\bar{\bar{F}}^i_{i,y} - \bar{S}_{i+1}\bar{\bar{F}}^{i+1}_{i+1,y} \\
&= \bar{S}_iK\left(\bar{q}^{i-1} - M^{i-1}\right)\bar{\bar{f}}^{i-1}_{i-1,z} + \bar{C}_{i+1}K(M^i - \bar{q}^i)\bar{\bar{f}}^i_{i,z} + \bar{D}^i_y, \quad n = 1, 2, 3, \ldots.
\end{aligned} \tag{121}$$

In the special case of interface m when $m > 1$, Eqs. (108) and (109) inserted in Eq. (107) give

$$\begin{aligned}
&-\bar{S}_m\bar{q}^{m-1}\bar{\bar{F}}^{m-1}_{m-1,y} + \left(\bar{C}_m + \bar{C}_{m+1}\bar{q}^m\right)\bar{\bar{F}}^m_{m,y} = \bar{S}_{m+1}\bar{\bar{F}}^{m+1}_{m+1,y} \\
&+\bar{S}_mK\left(\bar{q}^{m-1} - M^{m-1}\right)\bar{\bar{f}}^{m-1}_{m-1,z} + \bar{C}_{m+1}K\left(M^m - \bar{q}^m\right)\bar{\bar{f}}^m_{m,z} + \bar{D}^m_y, \quad n = 1, 2, 3, \ldots.
\end{aligned} \tag{122}$$

For each mode with $n > 0$, the linear equation system of Eq. (107) for all internal material interfaces can be written as

$$\bar{\mathcal{A}}\bar{\bar{\mathbf{F}}}_{\mathbf{y}} = \bar{\mathbf{h}}_{\mathbf{y}} \tag{123}$$

where $\bar{\mathcal{A}}$ is a matrix with $m \times m$ elements that can be identified with the coefficients on the left hand sides of Eqs. (120)–(122), $\bar{\bar{\mathbf{F}}}_{\mathbf{y}}$ is a vector with m elements containing the lower material numbered Fourier coefficients with subscript y for each internal material interface, and $\bar{\mathbf{h}}_y$ is a vector with m elements containing the known right hand sides of Eqs. (120)–(122). The tridiagonal structure of $\bar{\mathcal{A}}$ can be illustrated by the case of $m = 4$. In this case, Eq. (123) can be written as

$$\begin{bmatrix} \bar{a}_{11} & \bar{a}_{12} & 0 & 0 \\ \bar{a}_{21} & \bar{a}_{22} & \bar{a}_{23} & 0 \\ 0 & \bar{a}_{32} & \bar{a}_{33} & \bar{a}_{34} \\ 0 & 0 & \bar{a}_{43} & \bar{a}_{44} \end{bmatrix} \begin{bmatrix} \bar{\bar{F}}^1_{1,y} \\ \bar{\bar{F}}^2_{2,y} \\ \bar{\bar{F}}^3_{3,y} \\ \bar{\bar{F}}^4_{4,y} \end{bmatrix} = \begin{bmatrix} \bar{h}^1_y \\ \bar{h}^2_y \\ \bar{h}^3_y \\ \bar{h}^4_y \end{bmatrix} \tag{124}$$

3. COMPARISONS BETWEEN FOURIER SERIES AND FINITE ELEMENT ANALYSIS IN THE CASE OF A LAMINATE OF TWO INFINITELY LONG, CONDUCTING PLATES

3.1. Methods

MATLAB 2015b [10] and the harmonic eddy current solver in the FEA software ANSYS Maxwell 2015.1.0 (within Electromagnetics Suite 16.1.0) [11] have been used for comparisons with the analytical expressions. In the FEA without moving parts, the electromagnetic waves have been generated by the currents in 18 conductor bars, one per 10 electrical degrees, along the laminate, as shown in Fig. 4.

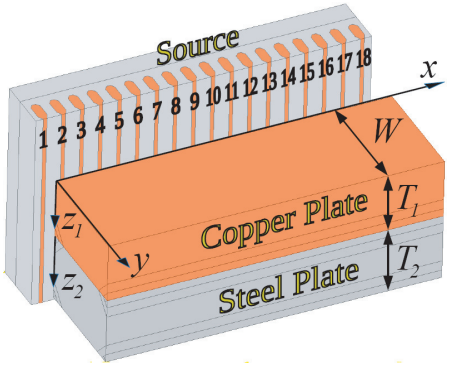

Figure 4. Geometry of a FE model of one 90 mm long part of a magnetic field source and a laminate of two plates with thicknesses $T_1 = 16$ mm and $T_2 = 18$ mm. The laminate width is 30 mm but W in the formulas is less than the width if boundary data are taken from locations within the laminate. Current bars are numbered 1–18.

The current in bar number ι is $i_\iota(t) = \widehat{i}\cos(\omega t - 5° - (\iota - 1)\cdot 10°)$ with $\widehat{i} = 100$ A. The source is separated from the laminate by 12 mm air gap. That is large enough for the $\bar{\mathbf{H}}$ components to be approximately sinusoidally distributed in the x direction in the laminate. The source current distribution can be approximated by

$$i(x,t) = \widehat{i}\cos(\omega t - kx). \tag{125}$$

This current has been used as a reference signal for the phase of $\bar{\mathbf{H}}$ and $\bar{\mathbf{E}}$ components in the laminate. The $\bar{\mathbf{H}}$ and $\bar{\mathbf{E}}$ components in the laminate can also be expressed as an amplitude multiplied by a cosine function. With $i = x$, y or z, component H_i is

$$H_i(x,y,z,t) = \widehat{H}_i(y,z)\cos(\omega t - kx + \varphi_i(y,z)). \tag{126}$$

Consequently, $\varphi_i(y,z)$ is a phase angle relative to the source current given by Eq. (125). The phase angle is negative if H_i lags i. Because of the harmonic variation, the amplitude and phase of a field component in a point in the laminate or on its boundary can be calculated from the instantaneous values $\pi/2$ apart. The amplitude is

$$\widehat{H}_i(y,z) = \sqrt{H_i^2(x,y,z,t) + H_i^2\left(x,y,z,t+\frac{\pi}{2\omega}\right)}. \tag{127}$$

Since $H_i(0,y,z,\frac{\pi}{2\omega}) = -\widehat{H}_i(y,z)\sin\varphi_i(y,z)$, Eq. (126) at $x=0$, with $\varphi_i(y,z)$ chosen to be within $[-\pi,\pi]$, gives

$$\varphi_i(y,z) = \begin{cases} \arccos\dfrac{H_i(0,y,z,0)}{\widehat{H}_i(y,z)} & \text{if } H_i\left(0,y,z,\dfrac{\pi}{2\omega}\right) \le 0 \\ -\arccos\dfrac{H_i(0,y,z,0)}{\widehat{H}_i(y,z)} & \text{if } H_i\left(0,y,z,\dfrac{\pi}{2\omega}\right) > 0 \end{cases}. \tag{128}$$

Field components and eddy current loss density have been evaluated along lines at constant x on the boundaries and in the interior of the laminate in the FE model. A way to increase the accuracy with a given FE mesh is to calculate averages in small boxes along the mentioned lines of evaluation. A faster way is to skip the boxes and calculate averages between lines at different x with the phase differences between the lines taken into consideration. This is based on the observation that, with an ideal FE mesh, a field component should be the same at (x,y,z,t) and $(x+\Delta x,y,z,t+\Delta t)$ with $\Delta t = k\Delta x/\omega$ since the laminate cross section at constant x is independent of x.

MATLAB has been used for calculation of 1: the amplitude and phase of the external boundary functions, 2: smooth functions, as explained below, that fit the real and imaginary parts of the external boundary functions, 3: the Fourier coefficients of the smooth functions, 4: the interface integrals, 5: the Fourier coefficients of the internal boundary functions, and 6: $\bar{\mathbf{H}}$ components, $\bar{\mathbf{E}}$ components and p along selected lines within the plates.

According to the sampling theorem, a band limited function with a shortest wave length $\lambda_{\min}$ can be reconstructed by function values at spatial points that are strictly less than $\lambda_{\min}/2$ apart. Consequently, Fourier coefficients of higher harmonics cannot be accurately calculated if only the values of field components in the rather few sample points along the evaluation lines are used. Therefore, smoothing splines and, for abruptly changing functions, shape preserving piecewise cubic polynomials have been fitted to values of the real and imaginary parts of each boundary function along the evaluation lines. The Fourier series of the field components have been approximated by up to 901 terms but 600 terms are sufficient to get very good agreement between FEA and Fourier series in the whole plates if both are non-magnetic. With plates of different permeability, the continuity condition of $\bar{B}_z$ and especially $\bar{H}_y$ were badly satisfied within two finite element lengths from the plate edges, although finite elements of higher order than default were used. Higher order elements had to be specified in the analysis options in the FEA in order to make the tangential $\bar{\mathbf{E}}$ components continuous across the interface between the plates and interfaces between plate parts of the same material but with different FE sizes.

A requirement for calculation of normal derivatives according to Subsection 2.2.1 is that boundary values of $\bar{\mathbf{E}}$ are available. However, the eddy current solver in ANSYS Maxwell 3D was not intended for calculation of useful $\bar{\mathbf{E}}$ values outside conducting materials when this work was done. Therefore, the laminate materials were chosen to be conductors, oxygen free copper with conductivity 58.5 MS/m in the top plate, and more or less cold worked stainless steel 201 L with conductivity 1.5 MS/m and relative permeability 1, 2 or 36 [12] in the bottom plate. The annealed condition gives the non-magnetic steel. The relative permeability in the source core is 8000. All the boundary values were taken from inside the laminate, typically 10–100 nm from the boundaries. In the case with relative permeability 36 in the bottom plate, field data were taken from $y = 0.8$ mm instead of $y = 0$, and from $y = 29.2$ mm instead of $y = 30$ mm because of the bad accuracy of the FEA closest to the edges of the magnetic plate. In this case, $W = 28.4$ mm in the analytical expressions.

3.2. Results

Chosen for plotting is the case with relative permeability 36 in the bottom plate. The continuous curves in each figure are from the Fourier series. The discrete plot symbols are FEA results. Fig. 5 and 6 show the amplitude of components of $\bar{\mathbf{H}}$ and $\bar{\mathbf{E}}$, respectively, along selected lines in the plates. The lines at constant z have been chosen to be relatively close to the interface between the plates since the results along these lines are relatively sensitive to the satisfaction of the continuity conditions at the interface between the plates. Fig. 7 shows the time averaged eddy current loss density along the selected lines. The purpose of the plots is just to show the agreement between FEA and Fourier series.

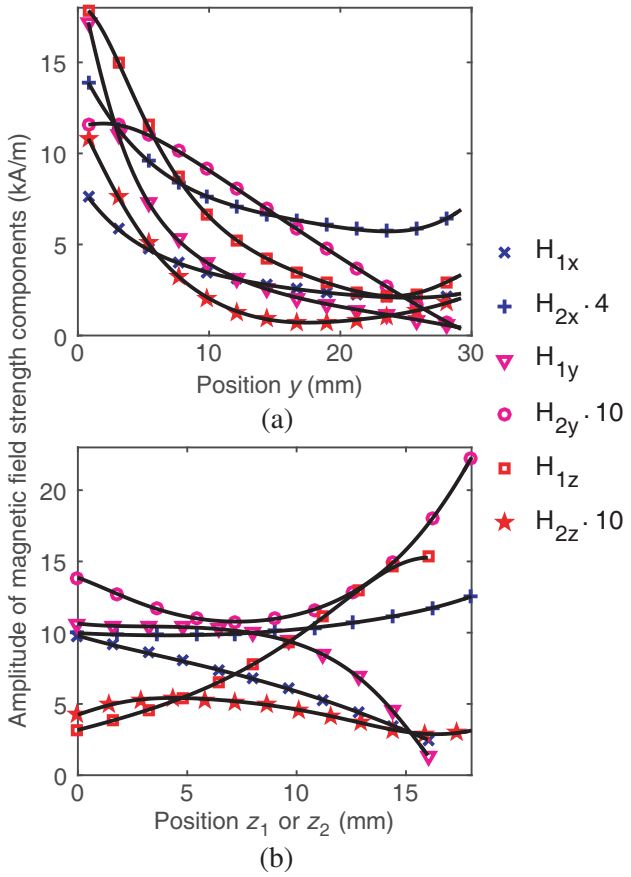

Figure 5. Amplitudes of components of magnetic field strength versus (a) y at $z_1 = 12\,\text{mm}$ in the copper plate and at $z_2 = 5\,\text{mm}$ in the steel plate, and (b) z_1 or z_2 at $y = 5\,\text{mm}$ in both plates. The continuous curves show the values of Fourier series. The discrete plot symbols mark FEA results.

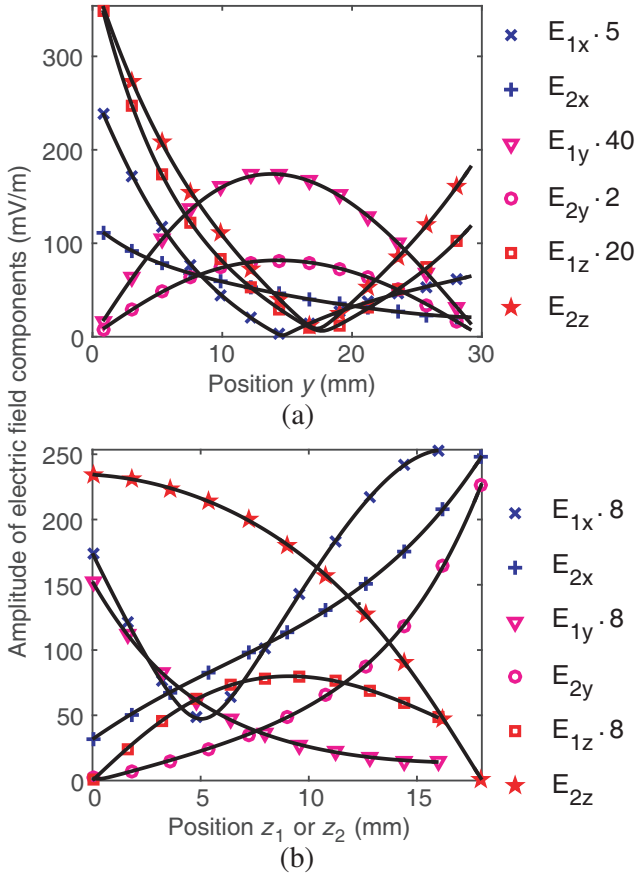

Figure 6. Amplitudes of components of electric field strength versus (a) y at $z_1 = 12\,\text{mm}$ in the copper plate and at $z_2 = 5\,\text{mm}$ in the steel plate, and (b) z_1 or z_2 at $y = 5\,\text{mm}$ in both plates. The continuous curves show the values of Fourier series. The discrete plot symbols mark FEA results.

4. DISCUSSION

One of the conclusions in [6] is that there is a surface current density on the material interfaces in a laminate as a consequence of the deposition of charges caused by the normal component of the total current density. If a charge can reach the surface of a conducting plate, it seems reasonable that it can also slide on the surface. However, Ampère's law and the continuity of the normal component of the total current density imply that a surface current density, if it exists, must be divergence free. Hence,

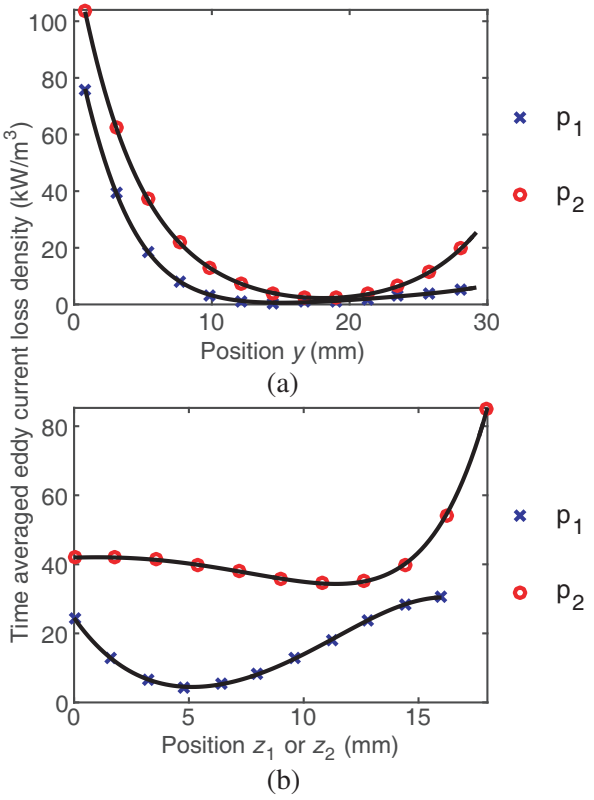

Figure 7. Time average of eddy current loss density versus (a) y at $z_1 = 12\,\text{mm}$ in the copper plate and at $z_2 = 5\,\text{mm}$ in the steel plate, and (b) z_1 or z_2 at $y = 5\,\text{mm}$ in both plates. The continuous curves show the values of Fourier series. The discrete plot symbols mark FEA results.

the surface current density is source free and cannot get any contribution from charges from the interior of the laminate plates and is not a consequence of capacitive effects. Hence, the volume current density along the material interface has finite values all the way out to and across the interface. Even if it would be possible to redirect the small normal component of current to a tangential direction at the material interfaces, the resulting surface current density would be negligible compared to $\mathbf{H}$ in a laminated core of, e.g., a conventional power generator operating at power grid frequency. Because of the continuity of $\bar{J}_{tot,z}$ and the low conductivity of the dielectric, almost all the induced voltage from the main pole flux in the laminate appears across the dielectric layers. An estimate of $\widehat{E}_{dielectric,z}$ can be obtained from the integral form of Eq. (4) applied to half a wave length of the laminate. Laminate stacking factor 0.95, $\omega = 100\pi\,\text{rad/s}$ and a pole flux amplitude of $1\,\text{Vs}$ through a square with area $1\,\text{m}^2$ gives $\widehat{E}_{dielectric,z} \approx 3.14\,\text{kV/m}$. The amplitude of $\bar{J}_{tot,z}$ at the interface between a conductor and a dielectric can be estimated by $\omega\varepsilon\widehat{E}_{dielectric,z} \approx 31\,\mu\text{A/m}^2$ if the dielectric is epoxy with relative permittivity 3.6. Therefore, in this article, the surface current density is assumed to be zero which implies that the tangential component of $\bar{\mathbf{H}}$ is continuous. This is correct for non-perfect conductors according to Cheng [9] and is used in ANSYS Maxwell.

The magnetic field concentration along the edges of magnetic plates can lead to local saturation along the edges. In that case, the precondition of uniform permeability in each plate is not fulfilled. The saturation makes the magnetic field less concentrated at the edges. This limits the usefulness of the derived Fourier series.

Mathematical expressions of Fourier series and propagation factors offer a mathematical explanation of the influence that lamination has on the electric and magnetic field components. The propagation factors can be dominated either by frequency and material properties or by plate dimensions and the pole pitch of the primary source of the electromagnetic field. For conducting plates with sufficiently

large width, thickness and length or pole pitch, the propagation factors are dominated by frequency and material properties, and the skin depth is approximately the well known $\delta = \sqrt{2/(\omega\mu\sigma)}$.

Demonstrated in this article is that each field component of an infinitely long, linear laminate can be expressed as the sum of two Fourier series. The two series are here referred to as the $\bar{\eta}_n$ series and the $\bar{\nu}_l$ series. In the special case when the thickness of a material layer is small, ξ_l is large. This makes the $\bar{\nu}_l$ series decrease rapidly in the y direction, into the laminate, except for mode $l = 0$, if it exists. It exists if the Fourier series is expressed with cosine instead of sine eigenfunctions such as for $\bar{H}_{y2}$ in Eq. (71). If the plate thickness is much smaller than the plate width and the wave length along the laminate, a field component in most of the interior of the laminate becomes approximately the $\bar{\eta}_n$ series plus the zero mode term of the $\bar{\nu}_l$ series. In a numerical example of a large machine operating at 50 Hz with $k = 2\pi/m$, $T = 0.5$ mm and $W = 25$ cm, each term in a sine series like (34) at $y \in [0.001W, 0.999W]$ is smaller than 21% of its value at $y = 0$ or W.

5. CONCLUSIONS

The derived Fourier series make it possible to calculate the time harmonic, traveling electric and magnetic fields within a plate or laminate of isotropic materials from measured or calculated field values on the boundaries of the plate or laminate.

The values of three of the six Cartesian components of the magnetic and electric fields on each boundary surface are sufficient for the complete determination of the harmonically time varying electric and magnetic fields within the plate or laminate. Which three components that must be known on any particular surface of a laminate depends on the choice of combination of boundary conditions. For certain combinations of different Neumann and Dirichlet conditions on all four boundaries of an infinitely long, linear laminate with rectangular cross section, it is possible to use the method of separation of variables and the orthogonality of the eigenfunctions for electromagnetic field calculation.

Via integrals along a material interface in a laminate, the fields at the interface can be strongly affected by the laminate boundary values at the ends of the interface. Each field component of an infinitely long, linear laminate can be expressed as the sum of two Fourier series. In the special case when the plate thickness is much smaller than the plate width and the wave length along the laminate, one of the series, the $\bar{\nu}_l$ series, is negligible except near some boundaries and except for mode $l = 0$, if it exists. However, since the Fourier coefficients of the other series, the $\bar{\eta}_n$ series, depend on the $\bar{\nu}_l$ series, via interface integrals, Fourier coefficients of both series are needed for the calculation of the $\bar{\eta}_n$ series.

ACKNOWLEDGMENT

The research presented in this thesis was carried out as a part of "Swedish Hydropower Centre — SVC". SVC has been established by the Swedish Energy Agency, Elforsk and Svenska Kraftnät together with Luleå University of Technology, The Royal Institute of Technology, Chalmers University of Technology and Uppsala University.

REFERENCES

1. Curti, M., J. J. H. Paulides, and E. A. Lomonova, "An overview of analytical methods for magnetic field computation," *2015 Tenth International Conference on Ecological Vehicles and Renewable Energies (EVER)*, 1–7, March 2015.
2. De Mey, G., "A method for calculatinġ eddy currents in plates of arbitrary geometry," *Archiv für Elektrotechnik*, Vol. 56, No. 3, 137–140, May 1974, [Online], Available: http://dx.doi.org/10.1007/BF01543294.
3. Singh, A., "Analysis of eddy currents in a plate with unequal overhangs," *IEEE Transactions on Magnetics*, Vol. 12, No. 5, 560–563, September 1976.
4. Mukerji, S. K., M. George, M. B. Ramamurthy, and K. Asaduzzaman, "Eddy currents in solid rectangular cores," *Progress In Electromagnetics Research*, Vol. 7, 117–131, 2008.

5. Mukerji, S. K., M. George, M. B. Ramamurthy, and K. Asaduzzaman, "Eddy currents in laminated rectangular cores," *Progress In Electromagnetics Research*, Vol. 83, 435–445, 2008.
6. Mukerji, S. K., D. S. Srivastava, Y. P. Singh, and D. V. Avasthi, "Eddy current phenomena in laminated structures due to travelling electromagnetic fields," *Progress In Electromagnetics Research M*, Vol. 18, 159–169, 2011.
7. Brander, O., "Partiella differential ekvationer-en kurs i fysikens matematiska metoder," del B. Studentlitteratur, 1973.
8. Griffiths, D. J., *Introduction to Electrodynamics*, 3rd Edition, Pearson, Addison Wesley, 1999.
9. Cheng, D. K., *Field and Wave Electromagnetics*, 2nd Edition, Addison-Wesley Publishing Company, 1989.
10. Mathworks website, https://www.mathworks.com/, accessed May 30, 2017.
11. Ansys website, http://www.ansys.com/, accessed May 30, 2017.
12. Matweb website, http://matweb.com/search/AdvancedSearch.aspx, accessed February 16, 2017.